JPET Fast Forward. Published on March 21, 2019 as DOI: 10.1124/jpet.118.255752
This article has not been copyedited and formatted. The final version may differ from this version.

JPET # 255752

Combining Multiscale Experimental and Computational Systems Pharmacological Approaches to Overcome Resistance to HER2-targeted Therapy in Breast Cancer

Tanaya R. Vaidya[1], Anusha Ande[1], Sihem Ait-Oudhia

Center for Pharmacometrics and Systems Pharmacology, Department of Pharmaceutics, College of Pharmacy, University of Florida, Orlando, FL, 32827, U.S.A. (T.R.V., A.A., S.AO).

JPET Fast Forward. Published on March 21, 2019 as DOI: 10.1124/jpet.118.255752
This article has not been copyedited and formatted. The final version may differ from this version.

Running title: Triple Combination Therapy in Resistant HER2+ Breast Cancer

Corresponding author: Sihem Ait-Oudhia, MS., PharmD., PhD.

Center for Pharmacometrics and Systems Pharmacology, Department of Pharmaceutics, College of Pharmacy, University of Florida. Address: 6550 Sanger Road. Office #469. Orlando. Florida. 32827. USA. Tel: +1 407-313-7037. Fax: +1 407-313-7030. Email: sihem.bihorel@cop.ufl.edu.

Text pages: 53

Tables: 2

Figures: 6

References: 43

Words in Abstract: 245

Words in Introduction: 667

Words in Discussion: 1272 (including reference citations)

Non-standard Abbreviations:

2D, two-dimensional; **3DD,** three-dimensional and dynamic; **4E-BP1,** eukaryotic translation initiation factor 4E-binding protein 1; **ADCC,** antibody dependent cellular cytotoxicity; **Akt,** AKT8 virus oncogene cellular homolog; **BC,** Breast Cancer; **DE,** dasatinib+everolimus simultaneous treatment; **DMSO,** Dimethyl sulfoxide; **FBS,** fetal bovine serum; **HER2,** Human Epidermal Growth Factor Receptor Type-2; **IGF-1R,** insulin-like growth factor receptor type-1; **IRS-1,** insulin receptor substrate-1; **JNK,** Jun N-terminal kinase; **MAPK,** mitogen-activated protein kinase; **mTOR,** mammalian target of rapamycin; **mTORC1,** mammalian target of rapamycin complex 1;

P_DE, paclitaxel followed by dasatinib+everolimus sequential treatment; **pAkt,** phosphorylated Akt; **PDE,** paclitaxel+dasatinib+everolimus treatment; **PI3K,** phosphatidylinositol 3-kinase; **PK/PD,** pharmacokinetics and pharmacodynamics; **pmTOR,** phosphorylated mTOR; **pSrc,** phosphorylated Src; **QSP,** quantitative systems pharmacology; **S6K,** Ribosomal protein S6 kinase-1; **SFKs,** Src family kinases; **Src,** SRC proto-oncogene non-receptor tyrosine kinase; **STAT3,** signal transducer and activator of transcription 3; **TTR,** time to tumor re-growth; **VEGF,** vascular endothelial growth factor

Recommended section: Chemotherapy, Antibiotics, and Gene Therapy

ABSTRACT

Emergence of HER2 therapy resistance in HER2-positive breast cancer (BC) poses a major clinical challenge. The primary mechanisms of resistance include aberrant activation of the HER2 and *PI3K*/*Akt*/*mTOR* pathways. The existence of feedback loops in this pathway may engender resistance to targeted therapies such as everolimus, an *mTOR* inhibitor, resulting in a more aggressive form of refractory HER2+BC. Here, we hypothesize that a triple and sequential combination therapy of paclitaxel, a potent cytotoxic agent, prior to concomitant administration of dasatinib, a *Src* family kinase inhibitor, with everolimus, restores sensitivity to treatment in refractory HER2+BC. This was assessed by a combination of experimental and computational approaches. Quantitative systems pharmacological (QSP), pharmacokinetics (PK), and pharmacodynamics (PD) studies were conducted in static and three-dimensional and dynamic (3DD) cell culture systems using a HER2-positive cell line resistant to HER2 therapy, JIMT-1. Dynamic responses in cellular viability and key signaling proteins in the HER2 and *PI3K*/*Akt*/*mTOR* pathways were measured upon treatments with single drugs, combinations, and appropriate controls. A QSP-PK/PD model was developed and used to optimize the sequence and inter-dose interval of the three agents in the combination. The proposed sequential combination therapy demonstrated strong cytotoxic effects in JIMT-1 cells, and our models predicted the usefulness of this combination over prolonged durations in the 3DD setting. Our combined experimental and QSP-PK/PD modeling approach may serve as a useful screening tool in predicting clinical efficacy of combination therapies in oncology. Nonetheless, further *in vivo* human xenograft tumor studies are warranted.

Key words: Three dimensional and dynamic cell culture, quantitative systems pharmacology, pharmacokinetics, pharmacodynamics, resistant HER2+ breast cancer

INTRODUCTION

Human Epidermal Growth Factor Receptor Type-2 positive (HER2+) breast cancer (BC) is characterized by an overexpression of the HER2 receptor on the cell surface in approximately 25% of all breast cancers. It has been associated with poor prognosis, higher incidence of metastases, and a shorter overall survival as compared to most other BC subtypes (Loibl and Gianni, 2017). HER2-targeted therapies such as Trastuzumab (Herceptin™) and lapatinib (TYKERB®) have demonstrated improved clinical outcomes in HER2+ metastatic BC, however, innate and/or acquired treatment resistance may occur (Yarden, 2001; Pohlmann et al., 2009; Singh et al., 2014; Zhang et al., 2017). Resistance to HER2 therapy in HER2+BC patients has become a significant clinical unmet medical need, motivating the search for alternative treatment approaches to overcome resistance and prolong patients' survival. Here, we propose to re-sensitize and/or combat a difficult-to-treat BC that is refractory to HER2 therapy with novel combination therapy comprising three agents with distinct, but complementary mechanisms of action including, everolimus, dasatinib, and paclitaxel.

Everolimus is a small molecule inhibitor of the *mTORC1* protein complex in the *PI3K/Akt/mTOR* pathway (Houghton, 2010), aberrantly activated in HER2-positive cancers (Wilks, 2015). Everolimus exerts its anti-tumor effects through *mTORC1*-mediated dephosphorylation of *S6K1* and *4E-BP1*, causing signal blockade in the *PI3K/Akt/mTOR* pathway and inhibition of cellular proliferation (O'Brien et al., 2014). In contrast, the inhibition of *mTORC1* releases a feedback activation loop mediated by *IGF-1R* and the insulin receptor, and results in the activation of *IRS-1*, which in turn activates *Akt* located upstream of *mTORC1* (O'Reilly et al., 2006). Therefore, a second agent targeting a signaling protein upstream of *Akt* is needed to counter-regulate this feedback activation loop (Yori et al., 2014). One such targeted small molecule agent is dasatinib

(Araujo and Logothetis, 2010). Dasatinib is a multi-kinase inhibitor of *Src*, a proto-oncogene from the *Src* family kinases (SFKs), located upstream of *Akt*. It is responsible for regulating multiple cellular growth pathways via the signaling proteins *Akt*, *MAPK*, and *STAT3* (Chang and Wang, 2013). Its over-activation has been implicated in HER2+BC cells' resistance to trastuzumab and lapatinib (De Luca et al., 2014; Jin et al., 2017). The dual inhibition of *mTOR* and SFKs in a mouse model of HER2+BC efficaciously caused tumor regression via prevention of the *Akt* feedback activation loop, thus, supporting the hypothesis that combination of everolimus with dasatinib may be successful at combating treatment resistance in HER2+BC (Dehm and Bonham, 2004; Yori et al., 2014).

To further enhance the tumor inhibitory effects of everolimus and dasatinib, we selected paclitaxel as a standard cytotoxic agent. Paclitaxel cell-killing results from microtubule stabilization leading to mitotic arrest and subsequently cancer cell death (Horwitz, 1994). In ovarian granulosa tumor cells, paclitaxel in combination with dasatinib or *mTOR* inhibitors showed a synergistic growth inhibitory effect (Haltia et al., 2017). Thus, the potent cytotoxic activity of paclitaxel mediated by the activation of apoptotic pathways, increases the likelihood of achieving synergistic tumor cell-killing when used in combination with the proposed targeted cytostatic agents in refractory HER2+BC.

In the present work, we sought to evaluate the efficacy of our proposed triple combination therapy. We conducted *in vitro* cell culture studies in two dimensional (2D) static and three dimensional dynamic (3DD) settings using a HER2+BC cell line resistant to trastuzumab and lapatinib, JIMT-1 (Köninki et al., 2010). Concentration-response, time-dependent cell-killing and activity of key signaling proteins were examined upon exposure of JIMT-1 cells to single and combination therapies. A pharmacokinetic and pharmacodynamic (PK/PD) study was conducted

using a 3DD cell culture system (Ho et al., 2004; Toriniwa and Komiya, 2007; Ande et al., 2018). A quantitative systems pharmacology (QSP)-PK/PD model was developed and characterized well all observed data. The developed QSP-PK/PD model served as an *in silico* tool for simulations of optimized dosing regimens and inter-dose intervals of the three agents that best re-sensitize (or overcome) resistance in HER2+BC. Our strategy of combining experimental and computational modalities is promising and may enable predictions of the clinical efficacy of the proposed triple combination as well as other therapeutic strategies in oncology.

MATERIAL AND METHODS

Drugs and Reagents:

Paclitaxel, everolimus, and dasatinib were purchased from Selleck Chemicals (Houston, TX). The JIMT-1 cell line was purchased from American Type Culture Collection (ATCC, Manassas, VA). Cell culture reagents including Dulbecco's modified Eagle's medium (DMEM), sodium bicarbonate solution and nonessential amino acids solution were purchased from Corning Inc. (Tewksbury, MA). Fetal bovine serum and cell counting kit-8 (CCK-8) were purchased from Sigma-Aldrich Co. (St. Louis, MO). The Bicinchoninic Acid (BCA) protein assay kit and protease inhibitor cocktail were obtained from Thermo Fisher Scientific (Waltham, MA). Crystal violet nuclear dye and the 3DD cell culture (BelloCell®) system apparatus were purchased from Chemglass Life Sciences, Vineland, NJ. *Caspase-3* colorimetric assay kit for assessing *caspase-3* activity was purchased from Abcam (Cambridge, MA). The radioimmunoprecipitation assay (RIPA) buffer was obtained from Boston BioProducts, (Ashland, MA). Phospho-*Akt*, phospho-*Src* and phospho-*mTOR* protein assay kits were purchased from EMD Millipore (Billercia, MA). Quantitative protein assays were conducted using the MAGPIX® multiplexing instrument from

JPET Fast Forward. Published on March 21, 2019 as DOI: 10.1124/jpet.118.255752
This article has not been copyedited and formatted. The final version may differ from this version.

Luminex Corporation (Austin, TX). Colorimetric assays for cell viability and *caspase-3* activity were performed using a microplate spectrophotometer (BioTek instruments, Winooski, VT).

Two-Dimensional (2D) or Static Cell Culture Experiments:

Concentration-response relationships were examined *in vitro,* following exposure of JIMT-1 cells to paclitaxel, everolimus and dasatinib, as described previously (Ande et al., 2018). *Caspase-3* activity in JIMT-1 cells was measured over a time course of 0, 6, 12, 24, 48 and 72 h following exposure to 50 nM of paclitaxel, everolimus and dasatinib as single agents and combinations, using a colorimetric *caspase-3* assay kit from Abcam (Cambridge, MA), as per the manufacturer's instructions. Total and phosphorylated *Src*, *Akt* and *mTOR* proteins were measured over a period of 0, 1, 3, 6, 12, 24 and 48 h following exposure of JIMT-1 cells to single agents and combinations of agents, using protein assay kits from EMD Millipore (Billercia, MA), as per the manufacturer's protocols. Cell viability over a time course of 0, 24, 48, 72 and 96 h was measured using the CCK-8 kit (Sigma-Aldrich Co. (St. Louis, MO)), following exposure of JIMT-1 cells to the single agents as well as combinations.

Three-Dimensional and Dynamic (3DD) Cell Culture Experiments:

A PK/PD study was conducted in a novel 3DD cell culture system (BelloCell® system; **Supplemental Figure 1**), by exposing JIMT-1 cells to a triple combination of paclitaxel followed by sequential administration of dasatinib plus everolimus under dynamic conditions, as described previously (Ande et al., 2018). Briefly, the 3DD system is an oscillating bioreactor that allows for high population density culture of cells over long periods of time (15-20 days). It is a fluid flow system that allows drug concentrations to be varied over time to mimic animal/human PK. Additionally, PD biomarkers can be sampled and measured without perturbing the system as such

(Ho et al., 2004; Toriniwa and Komiya, 2007). In the present study, paclitaxel was administered as a 3 h continuous infusion at a rate of 3.75 µg/min, to achieve a peak concentration of approximately 50 nM, based on a preliminary pilot study. On the following day, everolimus and dasatinib were administered into the system simultaneously with a constant concentration maintained at 50 nM for 72 h, followed by a washout phase. PK samples were collected over a period of 96 h starting from day 0, for measurement of paclitaxel concentrations in the system. Paclitaxel concentrations were quantified using high-pressure liquid chromatography–tandem mass spectrometry (LC-MS/MS). JIMT-1 cell viability was assessed every 24-48 h throughout the duration of the study using a crystal violet nuclear dye counting kit (Chemglass Life Sciences, Vineland, NJ).

QSP model for protein and cellular responses from the 2D cell culture setting:

Key proteins in the signaling pathway of HER2-therapy resistant BC cells were identified, and their activity was measured *in vitro* over a time course, upon exposure of JIMT-1 cells to paclitaxel, dasatinib and everolimus as single agents and combinations. Model building was performed by characterization of protein dynamics and cellular responses following perturbation of protein activity in response to: 1) single agents: paclitaxel (P), dasatinib (D), and everolimus (E), 2) dual combination therapy DE, and 3) triple combination therapy PDE (simultaneous) and P_DE (sequential) as depicted in **Figure 1**. All measured proteins were characterized using turnover rate constants (system parameters) across all treatment arms, and protein perturbations due to various treatment regimens were characterized using transit compartment models with inhibition or stimulation coefficients (Sun and Jusko, 1998; Lobo and Balthasar, 2002), as applicable (drug-related parameters).

All mathematical modeling was performed using Monolix software version 2016R1 (Lixoft SAS, 2016).

JPET Fast Forward. Published on March 21, 2019 as DOI: 10.1124/jpet.118.255752
This article has not been copyedited and formatted. The final version may differ from this version.

1) Single agents:

Paclitaxel:

Model development for paclitaxel was initiated with phosphorylated *Akt* (*pAkt*) being inhibited through the use of a precursor pool indirect response model (Sharma et al., 1998). Inhibition of the *PI3K*/*Akt* pathway is implicated in paclitaxel-mediated cell death in BC cells via activation of c-Jun N-terminal kinases (*JNK*), leading to activation of the apoptotic machinery (Sunters et al., 2006). Moreover, aberrant activation of this pathway is characteristic of HER2-therapy resistant BC cells, making it a key pathway for examination of protein activity perturbations. Inhibition of *Akt* activity leads to the inhibition of its downstream protein, *mTOR*, via dephosphorylation, which in turn causes the inhibition of cell proliferation through inhibition of ribosomal *S6K*, as described previously. Inhibition of *Akt* activity was accounted for in the model through the inhibition of a hypothetical compartment, $Akt_{Ic,}$ upstream of *Akt*, which phosphorylates *Akt* (Chudasama et al., 2015; Vaidya et al., 2018). *Akt* protein activity, however, returns to its baseline after approximately 6 h (**Figure 2**). Therefore, a precursor pool based indirect response model was utilized to capture this trend, as depicted in the following equations:

$$\frac{d(Akt_{Ic})}{dt} = K_{inh}.\left(1 - (C_P.Ip)\right) - K_{inh}.Akt_{Ic} \qquad ; Akt_{Ic}(0) = 1 \qquad (1)$$

$$\frac{d\left(pre_{pAkt}\right)}{dt} = K_{Akt} - K_{Akt}.Akt_{Ic}.pre_{pAkt} \qquad ; pre_{pAkt}(0) = 1 \qquad (2)$$

$$\frac{dpAkt}{dt} = K_{Akt}.Akt_{Ic}.pre_{pAkt} - K_{Akt}.pAkt \qquad ; pAkt(0) = 1 \qquad (3)$$

JPET Fast Forward. Published on March 21, 2019 as DOI: 10.1124/jpet.118.255752
This article has not been copyedited and formatted. The final version may differ from this version.

where, pre_{pAkt} and *pAkt* represent the precursor pool compartment and *pAkt* compartment. K_{inh} is the turnover rate constant for the inhibitory compartment, $Akt_{Ic,}$ while K_{Akt} is the turnover rate constant for the precursor pool and *Akt* protein. C_P represents paclitaxel concentration (50 nM) and Ip represents the coefficient for its inhibitory effect on cancer cells. All protein dynamic data were normalized to the no-treatment control arm. Therefore, homeostasis was maintained for the control protein dynamic data at a level of 1 unit under unperturbed conditions to satisfy the law of mass balance. The initial conditions for all protein compartments were set at 1.

Further, the inhibitory effect of *pAkt* on *pmTOR* was described through the following equations. Two transit compartments were able to adequately describe the delay in signaling between *pAkt* and *pmTOR* proteins (Sun and Jusko, 1998; Lobo and Balthasar, 2002) as follows:

$$\frac{dK_{M1}}{dt} = \left(\frac{1}{\tau_{MP}}\right).\left((pAkt^{S1_P}) - K_{M1}\right) \quad ; K_{M1}(0) = 1 \quad (4)$$

$$\frac{dK_{M2}}{dt} = \left(\frac{1}{\tau_{MP}}\right).(K_{M1} - K_{M2}) \quad ; K_{M2}(0) = 1 \quad (5)$$

$$\frac{d(pre_{pmTOR})}{dt} = K_{mTOR} - K_{mTOR}.K_{M2}.pre_{pmTOR} \quad ; pre_{pmTOR}(0) = 1 \quad (6)$$

$$\frac{dpmTOR}{dt} = K_{mTOR}.K_{M2}.pre_{pmTOR} - K_{mTOR}.pmTOR \quad ; pmTOR(0) = 1 \quad (7)$$

where, K_{M1} and K_{M2} represent transit compartments and τ_{MP} represents the mean transit time for the delay of paclitaxel-mediated signaling between *pAkt* and *pmTOR*. K_{mTOR} represents the turnover rate constant for *pmTOR*, and S_{1P} represents the coefficient for inhibition of *mTOR* activity due to paclitaxel.

JPET Fast Forward. Published on March 21, 2019 as DOI: 10.1124/jpet.118.255752
This article has not been copyedited and formatted. The final version may differ from this version.

In addition, *caspase-3* (*Cas3* in the equations), the executioner of apoptosis, is activated in response to paclitaxel treatment. Its activity over time was captured well with three transit compartments as shown in equations 8-10, which lead to the production of active *caspase-3* described by a pre-cursor pool indirect response model (**Figure 1**). A negative retro-regulation loop from the active *caspase-3* compartment (*Cas3*) to the first transit compartment (K_{C1}) allowed to capture the tolerance phenomenon observed in *caspase-3* activity temporal profile (i.e., return to the baseline activity level for *Cas3* while JIMT-1 cells are still exposed to paclitaxel).

$$\frac{dK_{C1}}{dt} = \left(\frac{1}{\tau_{CP}}\right).\left(\left(\frac{1+((k_P.C_P)^{S2_P})}{Cas3^{S3_P}}\right) - K_{C1}\right) \qquad ;K_{C1}(0) = 1 \qquad (8)$$

$$\frac{dK_{C2}}{dt} = \left(\frac{1}{\tau_{CP}}\right).(K_{C1} - K_{C2}) \qquad ;K_{C2}(0) = 1 \qquad (9)$$

$$\frac{dK_{C3}}{dt} = \left(\frac{1}{\tau_{CP}}\right).(K_{C2} - K_{C3}) \qquad ;K_{C3}(0) = 1 \qquad (10)$$

$$\frac{dpre_{Cas3}}{dt} = K_{cas} - K_{cas}.pre_{Cas3}.K_{C3} \qquad ;pre_{Cas3}(0) = 1 \qquad (11)$$

$$\frac{dCas3}{dt} = K_{cas}.pre_{Cas3}.K_{C3} - K_{cas}.Cas3 \qquad ;Cas3(0) = 1 \qquad (12)$$

where, k_P and $S2_P$ represent the slope and exponent for stimulatory effect of paclitaxel on *caspase-3* activity and τ_{CP} represents the mean transit time for paclitaxel-mediated *caspase-3* activation signaling. K_{cas} represents the turnover rate constant for *caspase-3* activity and $S3_P$ represents the feedback coefficient for *caspase-3* activity.

The changes in protein activity were linked to JIMT-1 cellular response as follows:

$$\frac{dR}{dt} = (pmTOR^{S4_P}).kg.R - kd_P.R.(Cas3 - 1) \qquad ;R(0) = R_0 \qquad (13)$$

JPET Fast Forward. Published on March 21, 2019 as DOI: 10.1124/jpet.118.255752
This article has not been copyedited and formatted. The final version may differ from this version.

where, *R* represents cell viability response. R_0 represents initial number of cells at time 0. Since all data were normalized to the control arm, R_0 was equal to 1. In the 2D experimental studies, JIMT-1 cells exhibited an exponential pattern in their growth over time under control conditions (no-treatment). Therefore, *kg*, the first-order growth rate constant was used to quantify JIMT-1 cellular proliferation rate. The protein signal from the *pmTOR* compartment (Eq.7) influenced the inhibition of JIMT-1 cells growth and its effect was incorporated using the exponent $S4_P$. The kd_P parameter represents the death rate constant for JIMT-1 cells and was used to stimulate JIMT-1 cells death driven by *caspase-3* activity. The subscript "*P*" in the above set of equations stands for all paclitaxel associated parameters.

Dasatinib:

Protein modeling for Dasatinib included the inhibition of its target protein *pSrc* via dephosphorylation, followed by the inhibition of its downstream proteins *pAkt* and *pmTOR*, as described by the following equations:

$$\frac{dpre_{pSrc}}{dt} = K_{Src} - K_{Src}.pre_{pSrc}.\left(1 - (C_D.S1_D)\right) \quad ; pre_{pSrc}(0) = 1 \qquad (14)$$

$$\frac{dpSrc}{dt} = K_{Src}.pre_{pSrc}.\left(1 - (C_D.S1_D)\right) - K_{Src}.pSrc \quad ; pSrc(0) = 1 \qquad (15)$$

$$\frac{dpre_{pAkt}}{dt} = K_{Akt} - K_{Akt}.pre_{pAkt} \qquad ; pre_{pAkt}(0) = 1 \qquad (16)$$

$$\frac{dpAkt}{dt} = K_{Akt}.pre_{pAkt} - K_{Akt}.\frac{pAkt}{pSrc^{S2_D}} \qquad ; pAkt(0) = 1 \qquad (17)$$

JPET Fast Forward. Published on March 21, 2019 as DOI: 10.1124/jpet.118.255752
This article has not been copyedited and formatted. The final version may differ from this version.

$$\frac{dK_{M1}}{dt} = \left(\frac{1}{\tau_{MD}}\right).\left((pAkt^{S3_D}) - K_{M1}\right) \quad ; K_{M1}(0) = 1 \quad (18)$$

$$\frac{dK_{M2}}{dt} = \left(\frac{1}{\tau_{MD}}\right).(K_{M1} - K_{M2}) \quad ; K_{M2}(0) = 1 \quad (19)$$

$$\frac{dpre_{pmTOR}}{dt} = K_{mtor} - K_{mtor}.K_{M2}.pre_{pmTOR} \quad ; pre_{pmTOR}(0) = 1 \quad (20)$$

$$\frac{dpmTOR}{dt} = K_{mtor}.K_{M2}.pre_{pmTOR} - K_{mtor}.pmTOR \quad ; pmTOR(0) = 1 \quad (21)$$

$$\frac{dR}{dt} = (pmTOR^{S4_D}).kg.R \quad ; R(0) = R_0 \quad (22)$$

A precursor pool-based indirect response model was used to capture *pSrc* inhibition under dasatinib treatment and to characterize the return to baseline phase after 9 h of *pSrc* inhibition (**Figure 2**). K_{Src} represents the turnover rate constant for *pSrc*, C_D is Dasatinib concentration (50 nM) and $S1_D$ is the coefficient for inhibition of *pSrc* due to Dasatinib effect. $S2_D$ represents the coefficient for effect of *pSrc* on *pAkt*, wherein *Akt* activity is inhibited via stimulation of loss of *pAkt* due to inhibition of *Src* (Liao and Hung, 2010). *mTOR* activity is then inhibited due to *pAkt* via two transit compartments, K_{M1} and K_{M2}, with τ_{MD} as the mean transit time and $S3_D$ as the coefficient of inhibition. The inhibition of *mTOR* activity drives the inhibition of JIMT-1 cellular response as shown in Eq. 22. The subscript "*D*" stands for all dasatinib associated parameters, and all other terms have the usual notations described previously.

Everolimus:

JPET Fast Forward. Published on March 21, 2019 as DOI: 10.1124/jpet.118.255752
This article has not been copyedited and formatted. The final version may differ from this version.

The final QSP model for everolimus integrated inhibition of the *pmTOR* protein, followed by a stimulatory feedback loop from *pmTOR* on the *pAkt* protein, in accordance with the reported literature and our observed *pAkt* activity data (**Figure 2**). Notably, an increase in *Src* activity in response to everolimus treatment was also observed. This is in line with the finding that rapamycin, an *mTOR*C1 inhibitor, causes phosphorylation and transactivation of the epidermal growth factor receptor (EGFR) pathway via *Src* activation in some cell lines, thus promoting cell survival (Chaturvedi et al., 2009). In addition, induction of IRS-1 and the release of feedback inhibition of the *IGF-1R*/*PI3K* pathway, causes *Akt* over-activation, which promotes cell growth in the presence of everolimus alone (O'Reilly et al., 2006). The model equations governing protein dynamics are as follows:

$$\frac{dpre_{pmTOR}}{dt} = K_{mtor} - K_{mtor}.pre_{pmTOR}.(1 - C_E.S1_E).(pAkt^{S2_E}) \quad ; pre_{pmTOR}(0) = 1 \quad (23)$$

$$\frac{dpmTOR}{dt} = K_{mtor}.pre_{pmTOR}.(1 - C_E.S1_E).(pAkt^{S2_E}) - K_{mtor}.pmTOR \; ; pmTOR(0) = 1 \quad (24)$$

$$\frac{dK_{S1}}{dt} = \left(\frac{1}{\tau_{SE}}\right).\left((pmTOR^{S3_E}) - K_{S1}\right) \quad ; K_{S1}(0) = 1 \quad (25)$$

$$\frac{dK_{S2}}{dt} = \left(\frac{1}{\tau_{SE}}\right).(K_{S1} - K_{S2}) \quad ; K_{S2}(0) = 1 \quad (26)$$

$$\frac{dK_{S3}}{dt} = \left(\frac{1}{\tau_{SE}}\right).(K_{S2} - K_{S3}) \quad ; K_{S3}(0) = 1 \quad (27)$$

$$\frac{dpre_{pSrc}}{dt} = K_{src} - K_{src}.\frac{pre_{pSrc}}{K_{S3}} \quad ; pre_{pSrc}(0) = 1 \quad (28)$$

$$\frac{dpSrc}{dt} = K_{src}.\frac{pre_{pSrc}}{K_{S3}} - K_{src}.pSrc \quad ; pSrc(0) = 1 \quad (29)$$

$$\frac{dpre_{pAkt}}{dt} = K_{Akt} - K_{Akt}.\frac{pre_{pAkt}}{pmTOR^{S4_E}} \quad ; pre_{pAkt}(0) = 1 \quad (30)$$

$$\frac{dpAkt}{dt} = K_{Akt}.\frac{pre_{pAkt}}{pmTOR^{S4_E}} - K_{Akt}.\frac{pAkt}{pSrc^{S5_E}} \quad ; pAkt(0) = 1 \quad (31)$$

JPET Fast Forward. Published on March 21, 2019 as DOI: 10.1124/jpet.118.255752
This article has not been copyedited and formatted. The final version may differ from this version.

$$\frac{dR}{dt} = (pmTOR^{S6_E}).kg.R \qquad ;R(0) = R_0 \qquad (32)$$

where C_E is everolimus concentration (50 nM) and $S1_E$ is everolimus coefficient of inhibition on *pmTOR*. Feedback activation of *pSrc* due to *pmTOR* was driven by three transit compartments. *pmTOR* activity drove the inhibition of proliferation of JIMT-1 cells as represented in Eq. 32. The subscript "E" denotes everolimus-associated model terms and parameters.

Of note, there was no increase in *caspase-3* activity observed in response to everolimus or dasatinib treatments, indicating a cytostatic effect of these two agents in JIMT-1 cells.

2) Dual combination therapy of dasatinib with everolimus (DE)

The dual therapy model included components of the individual models for each agent in the combination with attenuation of the feedback activation loops due to counter-regulatory mechanisms of dasatinib on everolimus. In addition, an active *caspase-3* component was included in the model due to slight elevation in active *caspase-3* expression observed with the dual combination (**Figure 3**). The corresponding model equations are as follows:

$$\frac{dpre_{pmTOR}}{dt} = K_{mtor} - K_{mtor}.pre_{pmTOR}.(1 - C_E.S1_E).(pAkt^{S1_{DE}}) \quad ;pre_{pmTOR}(0) = 1 \qquad (33)$$

$$\frac{dpmTOR}{dt} = K_{mtor}.pre_{pmTOR}.(1 - C_E.S1_E).(pAkt^{S1_{DE}}) - K_{mtor}.pmTOR \;\; ;pmTOR(0) = 1 \qquad (34)$$

$$\frac{dpre_{pSrc}}{dt} = K_{src} - K_{src}.pre_{pSrc}.\left(1 - (C_D.S1_D)\right) \qquad ;pre_{pSrc}(0) = 1 \qquad (35)$$

$$\frac{dpSrc}{dt} = K_{src}.pre_{pSrc}.\left(1 - (C_D.S1_D)\right) - K_{src}.pSrc \qquad ;pSrc(0) = 1 \qquad (36)$$

JPET Fast Forward. Published on March 21, 2019 as DOI: 10.1124/jpet.118.255752
This article has not been copyedited and formatted. The final version may differ from this version.

$$\frac{dpre_{pAkt}}{dt} = K_{Akt} - K_{Akt}.\frac{pre_{pAkt}}{pmTOR^{S4_E}} \quad ; pre_{pAkt}(0) = 1 \qquad (37)$$

$$\frac{dpAkt}{dt} = K_{Akt}.\frac{pre_{pAkt}}{pmTOR^{S4_E}} - K_{Akt}.\frac{pAkt}{pSrc^{S2_D}} \quad ; pAkt(0) = 1 \qquad (38)$$

$$\frac{dK_{C1}}{dt} = \left(\frac{1}{\tau_{CDE}}\right).\left(\left(\frac{1 + ((k_{DE}.C_{DE})^{S2_{DE}})}{Cas3}\right) - K_{C1}\right) \quad ; K_{C1}(0) = 1 \qquad (39)$$

$$\frac{dK_{C2}}{dt} = \left(\frac{1}{\tau_{CDE}}\right).\left(K_{C1}^{S3_{DE}} - K_{C2}\right) \quad ; K_{C2}(0) = 1 \qquad (40)$$

$$\frac{dpre_{Cas3}}{dt} = Kcas - Kcas.pre_{Cas3}.K_{C2} \quad ; pre_{Cas3}(0) = 1 \qquad (41)$$

$$\frac{dCas3}{dt} = Kcas.pre_{Cas3}.K_{C2} - K_{cas}.Cas3 \quad ; Cas3(0) = 1 \qquad (42)$$

$$\frac{dR}{dt} = (pmTOR^{S4_{DE}}).kg.R - kd_{DE}.R.(cas3 - 1) \quad ; R(0) = R_0 \qquad (43)$$

C_{DE} denotes concentration of dasatinib and everolimus (50 nM), and subscript "DE" denotes dasatinib-everolimus associated terms and parameters. $S1_{DE}$ is the coefficient for effect of *pAkt* on *pmTOR* in the presence of DE treatment. k_{DE} and $S2_{DE}$ are the slope and exponent for activation of *caspase-3* and τ_{CDE} is the mean transit time for delay in active *caspase-3* production. $S3_{DE}$ represents an exponent used for modulation of signaling intensity by amplification, to compensate for attenuation of signal due to time delays, required to characterize observed *caspase-3* activity (Sun and Jusko, 1998; Mager and Jusko, 2001). $S4_{DE}$ represents the coefficient of cell growth inhibition due to *pmTOR* with DE treatment and kd_{DE} is the cell death rate constant for JIMT-1 cells with DE treatment.

3) Triple combination therapy of paclitaxel with DE

JPET Fast Forward. Published on March 21, 2019 as DOI: 10.1124/jpet.118.255752
This article has not been copyedited and formatted. The final version may differ from this version.

QSP models were built to characterize the effect of PDE and P_DE treatments on selected proteins and JIMT-1 cells. PDE refers to concomitant administration of paclitaxel with DE, whereas, P_DE refers to paclitaxel administered 24 h prior to DE. The final combination QSP models integrated components from the individual agent QSP models with attenuation of feedback activation loops on *Src* and *Akt*. The mathematical equations for PDE treatment are as follows:

$$\frac{dpre_{pmTOR}}{dt} = K_{mtor} - K_{mtor}.pre_{pmTOR}.(1 - C_E.S1_E).(pAkt^{S1_{PDE}}) \quad ; pre_{pmTOR}(0) = 1 \tag{44}$$

$$\frac{dpmTOR}{dt} = K_{mtor}.pre_{pmTOR}.(1 - C_E.S_E).(pAkt^{S1_{PDE}}) - K_{mtor}.pmTOR \; ; pmTOR(0) = 1 \tag{45}$$

$$\frac{dpre_{pSrc}}{dt} = K_{src} - K_{src}.pre_{pSrc}.\left(1 - (C_D.S1_D)\right) \quad ; pre_{pSrc}(0) = 1 \tag{46}$$

$$\frac{dpSrc}{dt} = K_{src}.pre_{pSrc}.\left(1 - (C_D.S1_D)\right) - K_{src}.pSrc \quad ; pSrc(0) = 1 \tag{47}$$

$$\frac{d(Akt_{Ic})}{dt} = K_{inh}.\left(1 - (C_P.Ip)\right) - K_{inh}.Akt_{Ic} \quad ; Akt_{Ic}(0) = 1 \tag{48}$$

$$\frac{d\left(pre_{pAkt}\right)}{dt} = K_{Akt} - K_{Akt}.Akt_{Ic}.\frac{pre_{pAkt}}{pmTOR^{S2_{PDE}}} \quad ; pre_{pAkt}(0) = 1 \tag{49}$$

$$\frac{dpAkt}{dt} = K_{Akt}.Akt_{Ic}.\frac{pre_{pAkt}}{pmTOR^{S2_{PDE}}} - K_{Akt}.\frac{pAkt}{pSrc^{S2_D}} \quad ; pAkt(0) = 1 \tag{50}$$

$$\frac{dK_{C1}}{dt} = \left(\frac{1}{\tau_{CPDE}}\right).\left(\left(\frac{1 + ((k_{DE}.C_{DE})^{S2_{DE}}) + ((k_P.C_P)^{S2_P})}{Cas3}\right) - K_{C1}\right) \quad ; K_{CP1}(0) = 1 \tag{51}$$

$$\frac{dK_{C2}}{dt} = \left(\frac{1}{\tau_{CPDE}}\right).(K_{C1} - K_{C2}) \quad ; K_{CP2}(0) = 1 \tag{52}$$

JPET Fast Forward. Published on March 21, 2019 as DOI: 10.1124/jpet.118.255752
This article has not been copyedited and formatted. The final version may differ from this version.

$$\frac{dK_{C3}}{dt} = \left(\frac{1}{\tau_{CPDE}}\right).(K_{C2} - K_{C3}) \qquad ; K_{CP2}(0) = 1 \qquad (53)$$

$$\frac{dpre_{Cas3}}{dt} = Kcas - Kcas.pre_{Cas3}.K_{C3} \qquad ; pre_{Cas3}(0) = 1 \qquad (54)$$

$$\frac{dCas3}{dt} = Kcas.pre_{Cas3}.K_{C3} - K_{cas}.Cas3 \qquad ; Cas3(0) = 1 \qquad (55)$$

$$\frac{dR}{dt} = (pmTOR^{S3_{PDE}}).kg.R - kd_{PDE}.R.(cas3 - 1) \qquad ; R(0) = R_0 \qquad (56)$$

where $S1_{PDE}$ represents the effect of *pAkt* on *pmTOR* and $S2_{PDE}$ represents the coefficient for feedback activation of *pAkt* due to *pmTOR* in the presence of PDE treatment. $S3_{PDE}$ represents the coefficient of inhibition of cell growth due to *mTOR* activity and τ_{PDE} represents the mean transit time for activation of *caspase-3*. The subscript "PDE" denotes paclitaxel+dasatinib+everolimus associated terms and parameters.

The mathematical equations for the sequential combination P_DE are as follows:

For time < 24 h

$$\frac{d(Akt_{Ic})}{dt} = K_{inh}.\left(1 - (C_P.Ip)\right) - K_{inh}.Akt_{Ic} \qquad ; Akt_{Ic}(0) = 1 \qquad (57)$$

$$\frac{d\left(pre_{pAkt}\right)}{dt} = K_{Akt} - K_{Akt}.Akt_{Ic}.pre_{pAkt} \qquad ; pre_{pAkt}(0) = 1 \qquad (58)$$

$$\frac{dpAkt}{dt} = K_{Akt}.Akt_{Ic}.pre_{pAkt} - K_{Akt}.pAkt \qquad ; pAkt(0) = 1 \qquad (59)$$

$$\frac{dK_{M1}}{dt} = \left(\frac{1}{\tau_{MP}}\right).\left((pAkt^{S1_P}) - K_{M1}\right) \qquad ; K_{M1}(0) = 1 \qquad (60)$$

JPET Fast Forward. Published on March 21, 2019 as DOI: 10.1124/jpet.118.255752
This article has not been copyedited and formatted. The final version may differ from this version.

$$\frac{dK_{M2}}{dt} = \left(\frac{1}{\tau_{MP}}\right).(K_{M1} - K_{M2}) \quad ; K_{M2}(0) = 1 \quad (61)$$

$$\frac{d(pre_{pmTOR})}{dt} = K_{mTOR} - K_{mTOR}.K_{M2}.pre_{pmTOR} \quad ; pre_{pmTOR}(0) = 1 \quad (62)$$

$$\frac{dpmTOR}{dt} = K_{mTOR}.K_{M2}.pre_{pmTOR} - K_{mTOR}.pmTOR \quad ; pmTOR(0) = 1 \quad (63)$$

$$\frac{dpre_{pSrc}}{dt} = K_{Src} - K_{Src}.pre_{pSrc} \quad ; pre_{pSrc}(0) = 1 \quad (64)$$

$$\frac{dpSrc}{dt} = K_{Src}.pre_{pSrc} - K_{Src}.pSrc \quad ; pSrc(0) = 1 \quad (65)$$

$$\frac{dK_{C1}}{dt} = \left(\frac{1}{\tau_{CP}}\right).\left(\left(\frac{1 + ((k_P.C_P)^{S2_P})}{Cas3^{S3P}}\right) - K_{C1}\right) \quad ; K_{C1}(0) = 1 \quad (66)$$

$$\frac{dK_{C2}}{dt} = \left(\frac{1}{\tau_{CP}}\right).(K_{C1} - K_{C2}) \quad ; K_{C2}(0) = 1 \quad (67)$$

$$\frac{dK_{C3}}{dt} = \left(\frac{1}{\tau_{CP}}\right).(K_{C2} - K_{C3}) \quad ; K_{C3}(0) = 1 \quad (68)$$

$$\frac{dpre_{Cas3}}{dt} = Kcas - Kcas.pre_{Cas3}.K_{C3} \quad ; pre_{Cas3}(0) = 1 \quad (69)$$

$$\frac{dCas3}{dt} = Kcas.pre_{Cas3}.K_{C3} - K_{cas}.Cas3 \quad ; Cas3(0) = 1 \quad (70)$$

$$\frac{dR}{dt} = (pmTOR^{S4_P}).kg.R - kd_P.R.(cas3 - 1) \quad ; R(0) = R_0 \quad (71)$$

For time >= 24 h

$$\frac{d(Akt_{Ic})}{dt} = K_{inh}.\left(1 - (C_P.Ip)\right) - K_{inh}.Akt_{Ic} \quad ; Akt_{Ic}(0) = 1 \quad (72)$$

JPET Fast Forward. Published on March 21, 2019 as DOI: 10.1124/jpet.118.255752
This article has not been copyedited and formatted. The final version may differ from this version.

$$\frac{d(pre_{pAkt})}{dt} = K_{Akt} - K_{Akt}.Akt_{Ic}.\frac{pre_{pAkt}}{pmTOR^{S2_{P(DE)}}} \quad ; pre_{pAkt}(0) = 1 \qquad (73)$$

$$\frac{dpAkt}{dt} = K_{Akt}.Akt_{Ic}.\frac{pre_{pAkt}}{pmTOR^{S2_{P(DE)}}} - K_{Akt}.\frac{pAkt}{pSrc^{S2_D}} \quad ; pAkt(0) = 1 \qquad (74)$$

$$\frac{dpre_{pmTOR}}{dt} = K_{mtor} - K_{mtor}.pre_{pmTOR}.(1 - C_E.S1_E).(pAkt^{S1_{P(DE)}}) \quad ; pre_{pmTOR}(0) = 1 \qquad (75)$$

$$\frac{dpmTOR}{dt} = K_{mtor}.pre_{pmTOR}.(1 - C_E.S1_E).(pAkt^{S1_{P(DE)}}) - K_{mtor}.pmTOR \quad ; pmTOR(0) = 1 \qquad (76)$$

$$\frac{dpre_{pSrc}}{dt} = K_{src} - K_{src}.pre_{pSrc}.\left(1 - (C_D.S1_D)\right) \quad ; pre_{pSrc}(0) = 1 \qquad (77)$$

$$\frac{dpSrc}{dt} = K_{src}.pre_{pSrc}.\left(1 - (C_D.S1_D)\right) - K_{src}.pSrc \quad ; pSrc(0) = 1 \qquad (78)$$

$$\frac{dK_{C1}}{dt} = \left(\frac{1}{\tau_{CPDE}}\right).\left(\left(\frac{1 + ((k_{DE}.C_{DE})^{S2_{DE}}) + ((k_P.C_P)^{S2_P})}{Cas3}\right) - K_{C1}\right) \quad ; K_{C1}(0) = 1 \qquad (79)$$

$$\frac{dK_{C2}}{dt} = \left(\frac{1}{\tau_{CPDE}}\right).(K_{C1} - K_{C2}) \quad ; K_{C2}(0) = 1 \qquad (80)$$

$$\frac{dK_{C3}}{dt} = \left(\frac{1}{\tau_{CPDE}}\right).(K_{C2} - K_{C3}) \quad ; K_{C3}(0) = 1 \qquad (81)$$

$$\frac{dpre_{Cas3}}{dt} = Kcas - Kcas.pre_{Cas3}.K_{C3} \quad ; pre_{Cas3}(0) = 1 \qquad (82)$$

$$\frac{dCas3}{dt} = Kcas.pre_{Cas3}.K_{C3} - K_{cas}.Cas3 \quad ; Cas3(0) = 1 \qquad (83)$$

$$\frac{dR}{dt} = (pmTOR^{S3_{PDE}}).kg.R - kd_{PDE}.R.(cas3 - 1) \quad ; R(0) = R_0 \qquad (84)$$

JPET Fast Forward. Published on March 21, 2019 as DOI: 10.1124/jpet.118.255752
This article has not been copyedited and formatted. The final version may differ from this version.

Prior to administration of DE (<24 h), the model equations for paclitaxel single agent were employed, whereas, after 24 h, the model equations for the PDE simultaneous model were utilized. The only difference between the P_DE and PDE model parameters is the coefficient for feedback activation of *pAkt* due to *pmTOR* ($S2_{P(DE)}$ and $S2_{PDE}$), and the coefficient for effect of *pAkt* on *pmTOR* ($S1_{P(DE)}$ and $S1_{PDE}$), as a result of different degrees of feedback signal attenuation with the two treatment regimens.

The key features of all the mathematical models in the 2D experimental setting are: 1.) All measured protein activities are characterized using precursor-pool based indirect response models, with common turnover rate constants across all treatment arms (system parameters). 2.) Data from all treatment arms were normalized to the no-treatment control arm. Thus, homeostasis is maintained for the protein dynamic data in the control arm at a value of one unit, so as to satisfy the law of mass balance, and all protein initial conditions are set to unity. 3.) Protein activity perturbations due to the various treatment arms are introduced with the help of stimulatory or inhibitory coefficients and transit compartments, as applicable (drug-related parameters).

QSP and PK/PD models for protein and cellular responses in the 3DD cell culture setting:

A PK/PD study was conducted in the 3DD cell culture system to assess the efficacy of the triple and sequential combination therapy in JIMT-1 cells, as described in our previously published work (Ande et al., 2018). Briefly, paclitaxel was administered as a 3 h short-term intravenous infusion on day 0. After 24 h, the combination DE was administered as a constant exposure for 72 h (day 1 to 4) at concentrations of 50 nM for each agent and a washout phase of the 3DD cell culture system followed. The measured PD variables included cellular responses from control (no-treatment) and P_DE treatment arms. Paclitaxel PK was described with a two-compartment mammillary model, whereas dasatinib and everolimus concentrations were simulated based on their

JPET Fast Forward. Published on March 21, 2019 as DOI: 10.1124/jpet.118.255752
This article has not been copyedited and formatted. The final version may differ from this version.

dosing regimens and the input and output flow rates of media into the 3DD cell culture system (**Supplemental Figure 2**). The QSP model for intracellular signaling proteins was structurally identical to that of the P_DE combination from the 2D setting (Eq. 57-84). In order to characterize JIMT-1 cell growth in the 3DD system, a hybrid model (Magni et al., 2006) comprising exponential and linear cell growth components was employed and modified to account for treatment effects as follows:

Prior to administration of DE (< 24 h), only paclitaxel action is accounted for as follows –

$$\frac{dR}{dt} = \frac{\lambda_0 . R . mTOR^{\alpha_P}}{\left(1 + \left(\frac{\lambda_0}{\lambda_1} . R\right)^{\Psi}\right)^{\frac{1}{\Psi}}} - \beta_P . \Delta\, Cas3 . R \qquad ; R(0) = R_0 \tag{85}$$

Post-24 h, the combined effect of P and DE is taken into account, as implemented in the 2D setting, as follows –

$$\frac{dR}{dt} = \frac{\lambda_0 . R . mTOR^{\alpha_{PDE}}}{\left(1 + \left(\frac{\lambda_0}{\lambda_1} . R\right)^{\Psi}\right)^{\frac{1}{\Psi}}} - \beta_{PDE} . \Delta\, Cas3 . R \qquad ; R(0) = R_0 \tag{86}$$

where, R is the number of tumor cells, λ_0 and λ_1 are rate constants describing the exponential and linear growth of JIMT-1 cells. Ψ is a factor that allows for the switch from the exponential to the linear growth as tumor cell number increases. α_P and α_{PDE} are the power coefficients associated with effect of *pmTOR* protein activity on the inhibition of cell growth pre- and post-24 hours, and β_P and β_{PDE} are the death rate constants for JIMT-1 cells associated with *caspase-3* protein activity pre-

and post-24 hours. ΔCas3 represents the change in *caspase-3* activity from its baseline and was used to drive the killing of JIMT-1 cells.

In order to translate JIMT-1 cells responses from the 2D to 3DD cell culture setting, the cell growth inhibition rate constants associated with *pmTOR* activity and the cell death rate constants associated with *caspase-3* activity in both systems were compared and their ratios were termed as "scaling factors". Moreover, comparison of the cell growth data between 2D and 3DD settings for the control (no-treatment) arm indicated that the first-order growth rate constants in both systems were nearly identical, hence demonstrating a direct translatability of the JIMT-1 cellular response from the 2D to 3DD cell culture system for the control (no-treatment) arm.

The scaling factors (α_P/kd_P, α_{PDE}/kd_{PDE}) and (β_P/kd_P, β_{PDE}/kd_{PDE}) were calculated by using estimates from the model fittings for the P_DE arm in the 3DD and 2D cell culture settings. These scaling factors were then used to determine cell growth inhibition and cell death coefficients for the other treatment arms in the 3DD system (using the parameter estimates obtained from their 2D-system models), which included – everolimus and dasatinib as single agents and combination, paclitaxel alone, and paclitaxel, dasatinib and everolimus as a simultaneous combination (PDE). The calculated coefficients were used to simulate cellular response in the 3DD setting for the above treatment arms, and their simulated profiles were compared with the sequential treatment (P_DE) arm model fitting.

The final QSP-PK/PD model from the 3DD cell culture system was used to simulate cellular responses under various treatment schedules that included: inter-dose intervals of 24, 48, 72, 96 and 120 h for the P_DE sequential combination and PDE and P_DE treatment combinations at half the concentration levels used for each agent (i.e., 25 nM for 72 h followed by washout). Additionally,

long-term JIMT-1 cellular responses for all treatment arms were simulated (up to 50 days). In order to evaluate the relative efficacy and duration of response of these treatment schedules, the time-course profiles were compared for the time to JIMT-1 cells re-growth after cessation of treatment.

RESULTS

The schematic representation of the mathematical model for the protein signaling networks and cellular response is depicted in **Figure 1**.

QSP models for protein dynamics and cellular response in the 2D cell culture setting:

Protein Dynamics

The protein signaling networks and their impact on JIMT-1 cellular responses were established based on knowledge of the mechanisms of action of each single agent and combinations, and the pattern of time course profiles of measured proteins expression from JIMT-1 cells exposed to the various treatments in the 2D cell-culture setting. The established protein network models were used to drive cell viability of JIMT-1 cells for all tested treatment arms.

A decline in *pAkt* and *pmTOR* expression levels was observed following treatment with paclitaxel, indicating a cell growth inhibitory effect, in addition to activation of *caspase-3*, leading to an apoptotic effect in JIMT-1 cells (**Figure 2**). JIMT-1 cells treatment with dasatinib led to a decline in the expression level of its pharmacological target, *pSrc*, and subsequently, a decline in downstream *pAkt* and *pmTOR* expression levels (**Figure 2**). Hence, *pmTOR* protein activity was used as the driver of dasatinib inhibitory effect on JIMT-1 cells growth. For everolimus, a decline in *pmTOR* protein activity was observed in accordance with its mechanism of action as represented in **figure 2**. Moreover, a feedback activation of *pAkt* was also observed in parallel, a phenomenon that is commonly observed in response to *pmTOR* inhibition in several tumor types through release

of feedback inhibition from upstream tyrosine kinase signaling pathways (O'Reilly et al., 2006). In addition, we observed an increase in the expression levels of *pSrc* in response to everolimus treatment, which also contributed to an increase in *pAkt* protein expression and cell growth (**Figure 2**). Notably, we did not observe any significant increase in *caspase-3* activity for dasatinib and everolimus as single agents, indicating their cytostatic role in the HER2-therapy resistant JIMT-1 cell line.

Figure 3 depicts the temporal changes in the signaling protein levels compared to control for all examined combination therapies, including DE, PDE (simultaneous), and P_DE (sequential). The dual and triple combination (DE, PDE and P_DE) model structures were built in a hierarchical manner by including components from the individual agents' model structures. For example, the DE model was an integration of the dasatinib and everolimus single agent models with suppression of the *pSrc* feedback activation loop and attenuation of the *pAkt* feedback activation loop when the two drugs were administered simultaneously. For the P_DE sequential model, components of the paclitaxel model were included at times earlier than 24 h, while components of the PDE model were used at times beyond 24 h when DE treatment was administered.

In the DE combination arm, both pharmacological targets for dasatinib (*pSrc*) and everolimus (*pmTOR*) declined over time. Similarly, a decline to levels below the initial baseline value of the *pAkt* protein was observed, confirming the hypothesis that dasatinib counter-regulates the feedback activation loop of *pAkt* upon inhibition of *pmTOR* by everolimus. In the DE-perturbed protein model, components of the dasatinib and everolimus single agents' protein models were integrated and their parameters were fixed in the combination model to test their ability at capturing protein trends in the DE treatment arm. The only parameter that was estimated in this integrated model was the coefficient for effect of *pAkt* on *pmTOR* ($S1_{DE}$), which was comparable with the

JPET Fast Forward. Published on March 21, 2019 as DOI: 10.1124/jpet.118.255752
This article has not been copyedited and formatted. The final version may differ from this version.

corresponding coefficient in the everolimus single agent model ($S2_E$): 1.36±0.46 vs. 1.42±0.11 (**Table 1**). This parameter was estimated and compared to the everolimus arm because, the two transit compartments describing the delay in effect on *pmTOR* due to *pAkt* in the dasatinib model (K_{M1} and K_{M2}) were eliminated in this model, as there was direct inhibition of *pmTOR* due to everolimus. Additionally, the feedback activation loop from *pmTOR* to *pSrc* was also eliminated in this model, as *pSrc* levels were comparable to the dasatinib single agent arm (**Figures 2 and 3**), indicating that dasatinib completely suppresses everolimus-mediated feedback activation of *pSrc*. The trends in protein dynamics for the DE arm were captured reasonably well, thus qualifying our dasatinib and everolimus single agent models. Finally, a slight elevation in the activity of *caspase-3* protein (apoptosis marker) was also observed in the DE dual treatment arm (**Figure 3**), which contributed to cell death in our cell viability model, in conjunction with the growth inhibitory effect due to *pmTOR*.

The simultaneous (PDE) and sequential (P_DE) combination treatment models invoked features of the single agents and DE dual therapy models. There was a decline in *pSrc*, *pAkt* and *pmTOR* expression levels observed for both treatment arms, with distinct phases of protein signaling pre- and post-24 h reflected in our observed data and model fittings for the sequential treatment arm (**Figure 3**). Moreover, active *caspase-3* levels were elevated above baseline with a relatively larger magnitude as compared to the DE dual therapy (~1.5 times) and paclitaxel treatment alone (~1.2 times), for both triple agent combinations (**Figures 2 and 3**). Additionally, in the PDE treatment arm, the onset of *caspase-3* activation was observed to be earlier (24 h) in comparison to the DE and P_DE treatment arms (48 h; **Figure 3**), due to the combined synergistic activity of all three agents simultaneously.

JPET Fast Forward. Published on March 21, 2019 as DOI: 10.1124/jpet.118.255752
This article has not been copyedited and formatted. The final version may differ from this version.

Cellular Response

The established models for protein networks were able to capture the observed data relatively well, and were used as drivers to characterize JIMT-1 cell viability (cellular response) over time for the various treatment arms.

Figure 4 represents JIMT-1 cellular response to all treatment arms. For paclitaxel, almost 70% of cell killing from baseline was observed at 72 h, indicating its significantly cytotoxic role, causing inhibition of cell growth and stimulation of cell death in JIMT-1 cells. A decline in the viability of JIMT-1 cells was observed in the dasatinib treatment arm as compared to the control arm, as well. This was captured with an inhibitory effect of the *pmTOR* protein on cell growth through the model parameter, $S4_D$ (**Eq. 22**). On the contrary, JIMT-1 cells viability did not decline in the everolimus treatment arm as compared to control. This result suggests the existence of a feedback activation loop from *pmTOR* to *pAkt* via proteins of key cell survival and growth pathways (*S6K, IGF-1R, PI3K, Src*), which confers very weak sensitivity of JIMT-1 cells to everolimus. For the DE treatment arm, we observed a higher magnitude of cell killing as compared to either agent alone, due to attenuation of the feedback activation loop of *pAkt* in the presence of this dual combination. However, 100% cell killing was not achieved, due to the predominantly cytostatic effect of this combination. For both the triple combination arms (PDE and P_DE), the cytotoxic effects reached 100% killing of JIMT-1 cells by 96 h, indicating superior efficacy of the triple combination compared to the single agent arms and to DE therapy. Not surprisingly, in the P_DE arm, DE treatment post paclitaxel administration led to a slight delay (of approximately 24 h) in JIMT-1 cell death, as compared to the PDE simultaneous treatment arm (**Figure 4**).

Model parameters obtained from modeling all the observed data collected in the 2D cell culture setting are summarized in **Table 1**. Parameters for all models (single and combination

JPET Fast Forward. Published on March 21, 2019 as DOI: 10.1124/jpet.118.255752
This article has not been copyedited and formatted. The final version may differ from this version.

therapies) were estimated with reasonable precision. Certain parameters in the models were fixed to improve model stability. For example, coefficients for the effect of certain proteins on others were fixed to 1, as direct/inverse proportionality (as applicable) was sufficient to characterize these effects. Fixing these parameters did not have any significant impact on model performance as it did not change parameter estimates, nor compromised the precision of the remaining estimated parameters. In the case of everolimus treatment, since it had practically no effect on JIMT-1 cell viability, the inhibitory coefficient for cell growth due to *mTOR* protein activity ($S6_E$) was fixed to a very low value of 0.001 (**Table 1**) identified from trials and errors. No change in the effect on cell growth inhibition was observed at magnitudes lower than this. Overall, the established models could adequately capture the observed data, with reasonable precision on parameter estimates.

QSP and PK/PD models for cellular responses in the 3DD cell culture setting:

Figure 5 depicts the time course profiles of JIMT-1 cell viability in 3DD cell culture setting for actual measurements and model fittings of control and P_DE treatment arms; along with simulated response profiles for various dosing regimens of single and combination therapies. A hybrid exponential and linear cell growth model could adequately describe the growth of JIMT-1 cells in the absence of treatment in the 3DD system, whereas in a 2D cell culture setting, an exponential model was sufficient to characterize JIMT-1 cell growth. The rate constants for the exponential cell growth in 2D and 3DD settings were similar in magnitude and determined at 0.009 vs 0.008 h^{-1} in 2D vs. 3DD (**Table 1**). This result supports at least in part the translatability of findings for JIMT-1 cells from a 2D to 3DD cell culture setting. Furthermore, the time course of JIMT-1 cells viability in the 3DD cell culture system was reasonably captured for both treatment arms, control and sequential triple combination, using our established protein network model as a driver for JIMT-1 cellular response (black and red solid lines). The coefficients for inhibition of

JPET Fast Forward. Published on March 21, 2019 as DOI: 10.1124/jpet.118.255752
This article has not been copyedited and formatted. The final version may differ from this version.

cell growth due to *mTOR* activity and stimulation of cell death due to *caspase-3* activity in the 2D and 3DD systems for the sequential treatment arm (**Table 1**) were compared. The cell growth inhibition and cell death coefficients were not significantly different between the two settings (with ratios of 1 and 1.07, respectively), indicating translatability of our 2D QSP models to the 3DD system. These ratios were used as scaling factors to simulate the time course profiles of JIMT-1 cells viability in the 3DD setting for the remaining treatment arms.

Dasatinib (green) and everolimus (blue) treatment arms demonstrated marginal decrease in JIMT-1 cell viability from the control, mainly due to their cytostatic effects, whereas DE treatment arm (orange) showed a significantly higher cell killing than either agent alone. The simulated time course profiles of JIMT-1 cells killing were more noticeable in the single agent paclitaxel treatment arms when it was administered at a concentration regimen mimicking dasatinib and everolimus (50 nM for 72 h followed by washout; yellow) and administered as per the 3DD experimental study design (3 h short-term infusion; pink). A comparison of the simulated response of JIMT-1 cells to PDE (purple dashed) and P_DE (red dashed) treatments with all three drugs administered at the same dose levels (50 nM for 72 h followed by washout), showed a comparable magnitude of cell killing (~ 1.2-fold greater maximum cell killing with the PDE simultaneous arm as compared to the P_DE sequential arm), with cell response approaching similar magnitudes at later time points (beyond ~ 200 h). This was an expected finding as the sequential combination causes a delay in onset of JIMT-1 cell death due to dose staggering, as opposed to the simultaneous regimen with all three agents exerting cytostatic and/or cytotoxic effects through distinct mechanisms of action at the same time. A similar phenomenon was also observed in the 2D system (**Figure 4**), thus corroborating our findings from the 3DD simulations and providing confidence in our scaled-up QSP-PK/PD model. Moreover, these results suggest potential for dose staggering of P and DE while

JPET Fast Forward. Published on March 21, 2019 as DOI: 10.1124/jpet.118.255752
This article has not been copyedited and formatted. The final version may differ from this version.

achieving similar efficacy as that of the PDE simultaneous treatment arm in HER2-therapy resistant BC.

Figure 6 depicts the simulated responses of JIMT-1 viability for various treatment schedules (**Fig. 6A**) and over a long-term treatment period of 50 days (**Fig. 6B**). The additional simulated treatment schedules included P_DE sequential treatment with inter-dose intervals of 24, 48, 72, 96 and 120 hours, with all three drugs administered at the same dose levels (50 nM for 72 h followed by washout), and PDE and P_DE (24 h interval) treatment combinations at half dose levels (25 nM for 72 h followed by washout). A slight delay was observed in the time to tumor re-growth (TTR) of tumor cells in the P_DE regimens for 48 and 72 h intervals (**Fig. 6A**, green and yellow dashed profiles) as compared to the PDE simultaneous regimen (purple dashed profile), while the magnitude of tumor cell killing was comparable. Beyond inter-dose intervals of 72 hours, however, the P_DE sequential treatment regimens were not as efficacious as the simultaneous PDE regimen (96 h interval; blue dashed profile and 120 h interval; orange dashed profile), indicating almost complete washout of paclitaxel before DE administration, thus minimizing overlapping synergistic effects of the three agents. Nonetheless, the TTR was significantly delayed as compared to paclitaxel or DE treatment alone. Notably, despite reduction in the dose levels by half, the PDE and P_DE triple combinations had significantly higher efficacy in JIMT-1 cells as compared to the single and dual agent arms (black and grey dashed profiles).

Figure 6B represents simulated JIMT-1 cell growth profiles over a longer period of time (50 days), till all growth curves became nearly parallel to one another. The calculated TTR of tumor cells exposed to the various dosing regimens are summarized in **Table 2.** The individual agents, dasatinib, everolimus and paclitaxel, and the dual agent (DE) treatment arm had a relatively shorter TTR as compared to the PDE triple combination regimens. The P_DE treatment arms with 48 and

72 hours inter-dose intervals showed the longest TTR, without loss of efficacy, as compared to the PDE treatment, suggesting a synergistic effect of all three agents in this time window. Moreover, a reduction in dose levels by half in the triple combinations yielded significantly higher efficacy in JIMT-1 cells as compared to the single agents, further corroborating the synergistic effect of these three drugs in overcoming resistance to HER2 and *mTOR* therapies in BC.

DISCUSSION

HER2+BC represents 25% of all BC cases and is associated with poor prognosis, high incidence of metastases, and low survival rates (Slamon et al., 1987; Burstein, 2005; Kennecke et al., 2010). Despite improved treatment outcomes with HER2-targeted therapies such as trastuzumab and lapatinib, innate and acquired resistance to therapy remains a major unmet medical need (Pohlmann et al., 2009; Arteaga et al., 2011; Zhang et al., 2017). Here, we propose the use of a triple combination therapy comprising two targeted small molecule agents, dasatinib and everolimus, in combination with a standard cytotoxic agent, paclitaxel, in order to overcome resistance to HER2 therapy in HER2+BC. Dasatinib and everolimus are inhibitors of *Src* and *mTOR*, two key signaling proteins of the *PI3K*/*Akt*/*mTOR* pathway and downstream of several transmembrane tyrosine kinase receptors involved in cell growth and proliferation. The over activation of *Src* and *mTOR* proteins has been implicated in nearly 50% of HER2+BC cases (Yori et al., 2014). This medical challenge presents an opportunity for achieving enhanced cytostasis through dual inhibition of these proteins. Moreover, pre-clinical studies with HER2+BC cell lines and animal models have showed the benefit of dual inhibition of *Src* and *mTOR* at intensifying cell growth inhibition (Park et al., 2012; Yori et al., 2014). Taking into account the benefit of combining dasatinib and everolimus treatment for enhanced cell growth inhibition, we also added a third agent

to the combination, paclitaxel, as an inducer of apoptosis, to augment the overall cytotoxic effect of our combination therapy.

In the present work, we tested the potential of our proposed triple combination therapy at overcoming resistance to HER2 therapy in the HER2-therapy resistant cell line, JIMT-1. A combined experimental and computational QSP approach was successfully applied for control, single, and combination therapies, where temporal changes in molecular (protein signaling) and cellular responses were measured in 2D and 3DD cell culture systems; and successfully characterized with QSP models. In the 2D *in vitro* setting, dasatinib as a single agent demonstrated a cytostatic effect through inhibition of the activity of *Src* protein followed by a decline in the *Akt* and *mTOR* protein activities, which led to inhibition of JIMT-1 cellular growth. Everolimus as a single agent, was inefficacious at inhibiting JIMT-1 cell growth at the concentrations tested, likely due to feedback activation of *Src* and *Akt* protein activities. Similar results have been previously reported on the weak sensitivity of JIMT-1 cells to everolimus (Dragowska et al., 2011). The combination of both agents successfully suppressed this feedback activation loop leading to a much higher cytostatic effect than either agent alone. This was an expected finding because, both agents target proteins in the aberrantly activated *Akt/mTOR* pathway in HER2-resistant BC cells through distinct mechanisms of action that are also complementary to each other. Moreover, a study reported on other BC cell lines having feedback activation of *Akt*, yielded similar results upon treatment with a combination of dasatinib and rapamycin, an *mTOR* inhibitor (Yori et al., 2014). The single agent paclitaxel showed both cytostatic and cytotoxic effects on JIMT-1 cells. This result is consistent with the mechanism of action of paclitaxel, causing microtubule disarray and cell cycle arrest followed by apoptosis (Horwitz, 1994) (Wang et al., 2000). Furthermore, the cytostatic effect due to paclitaxel can also be attributed to inhibition of a central cellular signaling and growth

protein, *Akt*, via dephosphorylation, as observed with our experimental data **(Figure 2)**, in accordance with literature findings (MacKeigan et al., 2002; Sunters et al., 2006).

In the 2D setting, both triple combinations PDE (simultaneous) and P_DE (sequential) showed strong cytotoxic effects on JIMT-1 cells reaching 100% cell killing at 96 h. Despite these comparable cytotoxicity effects of PDE and P_DE, only P_DE was further examined in our novel 3DD cell culture system (Ande et al., 2018). The rationale was twofold: First, prior treatment with paclitaxel is hypothesized to be particularly useful in the *in vivo* and/or clinical setting due to its tumor priming effect, through which it allows penetration of targeted agents and nanomedicines into the inner layers of solid tumors (Lu et al., 2007). Second, dose staggering of paclitaxel and the DE combination may provide a clinical safety benefit as to reducing the occurrence and/or intensity of potential common adverse events of these drugs, particularly hematologic toxicities such as neutropenia and thrombocytopenia (Fornier et al., 2011; Ocana et al., 2017; Toi et al., 2017). Our experimental results in the 3DD cell culture system show that P_DE treatment substantially blocks (8.5-fold compared to control) the growth of JIMT-1 cells in a durable manner lasting up to a time beyond cessation of therapy (up to 15 days). The latter result would not be possible to obtain from a 2D cell culture experiment due to the relatively short maximum duration of study design (~ 5 days) in this setting. Hence, our novel 3DD cell culture system presents several advantages over the traditional 2D cell culture system: first, ability for serial sampling of cells over a relatively long period of time (two or more weeks) for measurement of cellular response without significant perturbations in the system; second, the system provides a three-dimensional environment for growth of adherent cells, which is closer to an *in vivo* tumor environment than a standard 2D cell culture system; third, flexibility of adjusting drugs' dosing regimens in order to mimic animal or human PK of drugs. This was used in our 3DD experiments, where PK of paclitaxel was simulated

along with a constant exposure to DE combination therapy. The subsequently measured PK and JIMT-1 cellular responses were well characterized with our scaled up QSP-PK/PD model.

The calculated scaling factors (from 2D to 3DD) and the initial JIMT-1 growth rate constants indicated similarities between both systems and supported translation and applicability of our QSP models from the 2D setting to the 3DD setting. Our simulations of the simultaneous (PDE) and sequential (P_DE) triple combinations (24, 48, 72 h inter-dose intervals) in the 3DD setting demonstrated similar magnitudes of cytotoxic effects, however with a slight delay in the onset of tumor cells re-growth for the P_DE treatment, as predicted by our long-term model simulations, thus providing an opportunity for dose staggering of P and DE. Moreover, despite dose reduction of the triple combinations, significant efficacy against JIMT-1 cells was retained as suggested by our model simulations, corroborating the synergistic effect of all three agents. The synergism can be largely attributed to DE-mediated targeted inhibition of the crucial *PI3K*/*Akt*/*mTOR* axis which is aberrantly activated in HER2-therapy resistant BC, making the cells particularly susceptible to this treatment combination. Furthermore, this can provide opportunities to reduce individual dose levels for all three agents when used in combination, minimizing potential occurrence of overlapping side-effects.

In summary, the superior efficacy of our proposed triple combination therapy of paclitaxel with dasatinib and everolimus at overcoming resistance to HER2-targeted therapies in BC is established *in vitro*. Our novel 3DD cell culture system allowed us to mimic the PK of the three agents, which influenced the dynamical changes in protein signaling and cellular responses of JIMT-1 cells. The final established QSP-PK/PD models were able to characterize cell viability in the 3DD system relatively well under the given treatment conditions, and were able to predict cellular responses to various other dosing regimens over a relatively long period of time. Thus, our

approach of combining the use of our novel 3DD cell culture system with the aid of QSP-PK/PD as a mathematical modeling and simulation tool has potential application for screening of successful combination therapies in oncology; and may serve as a surrogate for animal studies that may not be feasible in some cases and/or might not be representative of human systems.

Acknowledgements: The authors would like to acknowledge Ashley N. Brown and Michael Vicchiarelli (Department of Medicine, Institute for Therapeutic Innovation, University of Florida, Orlando, USA) and Bao N. Tran for technical assistance.

Authorship contributions:

Participated in research design: Tanaya R. Vaidya, Anusha Ande, Sihem Ait-Oudhia

Conducted experiments: Anusha Ande

Contributed new reagents or analytic tools: Tanaya R. Vaidya, Anusha Ande, Sihem Ait-Oudhia

Performed data analysis: Tanaya R. Vaidya, Anusha Ande, Sihem Ait-Oudhia

Wrote or contributed to the writing of the manuscript: Tanaya R. Vaidya, Anusha Ande, Sihem Ait-Oudhia

References

Ande A, Vaidya TR, Tran BN, Vicchiarelli M, Brown AN and Ait-Oudhia S (2018) Utility of a Novel Three-Dimensional and Dynamic (3DD) Cell Culture System for PK/PD Studies: Evaluation of a Triple Combination Therapy at Overcoming Anti-HER2 Treatment Resistance in Breast Cancer. *Front Pharmacol* **9**:403.

Araujo J and Logothetis C (2010) Dasatinib: a potent SRC inhibitor in clinical development for the treatment of solid tumors. *Cancer Treat Rev* **36**:492-500.

Arteaga CL, Sliwkowski MX, Osborne CK, Perez EA, Puglisi F and Gianni L (2011) Treatment of HER2-positive breast cancer: current status and future perspectives. *Nat Rev Clin Oncol* **9**:16-32.

Burstein (2005) The distinctive nature of HER2-positive breast cancers. *Perspective* **353**:1652-1655.

Chang AY and Wang M (2013) Molecular mechanisms of action and potential biomarkers of growth inhibition of dasatinib (BMS-354825) on hepatocellular carcinoma cells. *BMC Cancer* **13**:267.

Chaturvedi D, Gao X, Cohen MS, Taunton J and Patel TB (2009) Rapamycin induces transactivation of the EGFR and increases cell survival. *Oncogene* **28**:1187-1196.

Chudasama VL, Ovacik MA, Abernethy DR and Mager DE (2015) Logic-Based and Cellular Pharmacodynamic Modeling of Bortezomib Responses in U266 Human Myeloma Cells. *J Pharmacol Exp Ther* **354**:448-458.

De Luca A, D'Alessio A, Gallo M, Maiello MR, Bode AM and Normanno N (2014) Src and CXCR4 are involved in the invasiveness of breast cancer cells with acquired resistance to lapatinib. *Cell Cycle* **13**:148-156.

Dehm SM and Bonham K (2004) SRC gene expression in human cancer: the role of transcriptional activation. *Biochem Cell Biol* **82**:263-274.

Dragowska WH, Weppler SA, Qadir MA, Wong LY, Franssen Y, Baker JH, Kapanen AI, Kierkels GJ, Masin D, Minchinton AI, Gelmon KA and Bally MB (2011) The combination of gefitinib and RAD001 inhibits growth of HER2 overexpressing breast cancer cells and tumors irrespective of trastuzumab sensitivity. *BMC Cancer* **11**:420.

Fornier MN, Morris PG, Abbruzzi A, D'Andrea G, Gilewski T, Bromberg J, Dang C, Dickler M, Modi S, Seidman AD, Sklarin N, Chang J, Norton L and Hudis CA (2011) A phase I study of dasatinib and weekly paclitaxel for metastatic breast cancer. *Ann Oncol* **22**:2575-2581.

Haltia UM, Andersson N, Yadav B, Färkkilä A, Kulesskiy E, Kankainen M, Tang J, Bützow R, Riska A, Leminen A, Heikinheimo M, Kallioniemi O, Unkila-Kallio L, Wennerberg K, Aittokallio T and Anttonen M (2017) Systematic drug sensitivity testing reveals synergistic growth inhibition by dasatinib or mTOR inhibitors with paclitaxel in ovarian granulosa cell tumor cells. *Gynecol Oncol* **144**:621-630.

Ho L, Greene CL, Schmidt AW and Huang LH (2004) Cultivation of HEK 293 cell line and production of a member of the superfamily of G-protein coupled receptors for drug discovery applications using a highly efficient novel bioreactor. *Cytotechnology* **45**:117-123.

Horwitz SB (1994) Taxol (paclitaxel): mechanisms of action. *Ann Oncol* **5 Suppl 6**:S3-6.

Houghton PJ (2010) Everolimus. *Clin Cancer Res* **16**:1368-1372.

Jin MH, Nam AR, Park JE, Bang JH, Bang YJ and Oh DY (2017) Resistance Mechanism against Trastuzumab in HER2-Positive Cancer Cells and Its Negation by Src Inhibition. *Mol Cancer Ther* **16**:1145-1154.

Kennecke H, Yerushalmi R, Woods R, Cheang MC, Voduc D, Speers CH, Nielsen TO and Gelmon K (2010) Metastatic behavior of breast cancer subtypes. *J Clin Oncol* **28**:3271-3277.

Köninki K, Barok M, Tanner M, Staff S, Pitkänen J, Hemmilä P, Ilvesaro J and Isola J (2010) Multiple molecular mechanisms underlying trastuzumab and lapatinib resistance in JIMT-1 breast cancer cells. *Cancer Lett* **294**:211-219.

Liao Y and Hung MC (2010) Physiological regulation of Akt activity and stability. *Am J Transl Res* **2**:19-42.

Lobo ED and Balthasar JP (2002) Pharmacodynamic modeling of chemotherapeutic effects: application of a transit compartment model to characterize methotrexate effects in vitro. *AAPS pharmSci* **4**:E42.

Loibl S and Gianni L (2017) HER2-positive breast cancer. *Lancet* **389**:2415-2429.

Lu D, Wientjes MG, Lu Z and Au JL (2007) Tumor priming enhances delivery and efficacy of nanomedicines. *The Journal of pharmacology and experimental therapeutics* **322**:80-88.

MacKeigan JP, Taxman DJ, Hunter D, Earp HS, Graves LM and Ting JP (2002) Inactivation of the antiapoptotic phosphatidylinositol 3-kinase-Akt pathway by the combined treatment of taxol and mitogen-activated protein kinase kinase inhibition. *Clin Cancer Res* **8**:2091-2099.

Mager DE and Jusko WJ (2001) Pharmacodynamic modeling of time-dependent transduction systems. *Clinical pharmacology and therapeutics* **70**:210-216.

Magni P, Simeoni M, Poggesi I, Rocchetti M and De Nicolao G (2006) A mathematical model to study the effects of drugs administration on tumor growth dynamics. *Mathematical biosciences* **200**:127-151.

O'Brien NA, McDonald K, Tong L, von Euw E, Kalous O, Conklin D, Hurvitz SA, di Tomaso E, Schnell C, Linnartz R, Finn RS, Hirawat S and Slamon DJ (2014) Targeting PI3K/mTOR overcomes resistance to HER2-targeted therapy independent of feedback activation of AKT. *Clin Cancer Res* **20**:3507-3520.

O'Reilly KE, Rojo F, She QB, Solit D, Mills GB, Smith D, Lane H, Hofmann F, Hicklin DJ, Ludwig DL, Baselga J and Rosen N (2006) mTOR inhibition induces upstream receptor tyrosine kinase signaling and activates Akt. *Cancer Res* **66**:1500-1508.

Ocana A, Gil-Martin M, Martín M, Rojo F, Antolín S, Guerrero Á, Trigo JM, Muñoz M, Pandiella A, Diego NG, Bezares S, Caballero R, Carrasco E and Urruticoechea A (2017) A phase I study of the SRC kinase inhibitor dasatinib with trastuzumab and paclitaxel as first line therapy for patients with HER2-overexpressing advanced breast cancer. GEICAM/2010-04 study. *Oncotarget* **8**:73144-73153.

Park BJ, Whichard ZL and Corey SJ (2012) Dasatinib synergizes with both cytotoxic and signal transduction inhibitors in heterogeneous breast cancer cell lines--lessons for design of combination targeted therapy. *Cancer Lett* **320**:104-110.

Pohlmann PR, Mayer IA and Mernaugh R (2009) Resistance to Trastuzumab in Breast Cancer. *Clin Cancer Res* **15**:7479-7491.

Sharma A, Ebling WF and Jusko WJ (1998) Precursor-dependent indirect pharmacodynamic response model for tolerance and rebound phenomena. *J Pharm Sci* **87**:1577-1584.

Singh JC, Jhaveri K and Esteva FJ (2014) HER2-positive advanced breast cancer: optimizing patient outcomes and opportunities for drug development. *Br J Cancer* **111**:1888-1898.

Slamon DJ, Clark GM, Wong SG, Levin WJ, Ullrich A and McGuire WL (1987) Human breast cancer: correlation of relapse and survival with amplification of the HER-2/neu oncogene. *Science (New York, NY* **235**:177-182.

Sun YN and Jusko WJ (1998) Transit compartments versus gamma distribution function to model signal transduction processes in pharmacodynamics. *Journal of pharmaceutical sciences* **87**:732-737.

Sunters A, Madureira PA, Pomeranz KM, Aubert M, Brosens JJ, Cook SJ, Burgering BM, Coombes RC and Lam EW (2006) Paclitaxel-induced nuclear translocation of FOXO3a in breast cancer cells is mediated by c-Jun NH2-terminal kinase and Akt. *Cancer research* **66**:212-220.

Toi M, Shao Z, Hurvitz S, Tseng LM, Zhang Q, Shen K, Liu D, Feng J, Xu B, Wang X, Lee KS, Ng TY, Ridolfi A, Noel-Baron F, Ringeisen F and Jiang Z (2017) Efficacy and safety of everolimus in combination with trastuzumab and paclitaxel in Asian patients with HER2+ advanced breast cancer in BOLERO-1. *Breast Cancer Res* **19**:47.

Toriniwa H and Komiya T (2007) Japanese encephalitis virus production in Vero cells with serum-free medium using a novel oscillating bioreactor. *Biologicals* **35**:221-226.

Vaidya T, Kamta J, Chaar M, Ande A and Ait-Oudhia S (2018) Systems pharmacological analysis of mitochondrial cardiotoxicity induced by selected tyrosine kinase inhibitors. *J Pharmacokinet Pharmacodyn* **45**:401-418.

Wang TH, Wang HS and Soong YK (2000) Paclitaxel-induced cell death: where the cell cycle and apoptosis come together. *Cancer* **88**:2619-2628.

Wilks ST (2015) Potential of overcoming resistance to HER2-targeted therapies through the PI3K/Akt/mTOR pathway. *Breast* **24**:548-555.

Yarden Y (2001) Biology of HER2 and its importance in breast cancer. *Oncology* **61 Suppl 2**:1-13.

Yori JL, Lozada KL, Seachrist DD, Mosley JD, Abdul-Karim FW, Booth CN, Flask CA and Keri RA (2014) Combined SFK/mTOR inhibition prevents rapamycin-induced feedback activation of AKT and elicits efficient tumor regression. *Cancer Res* **74**:4762-4771.

Zhang L, Huang Y, Zhuo W, Zhu Y, Zhu B and Chen Z (2017) Identification and characterization of biomarkers and their functions for Lapatinib-resistant breast cancer. *Med Oncol* **34**:89.

Footnotes

Footnotes to authors:

[1] These authors contributed equally to the work.

Legend for Figures

Figure 1. Model structure for key protein signaling pathways affected by paclitaxel, dasatinib and everolimus as single agents and combinations in JIMT-1 breast cancer cells resistant to HER2-targeted therapy. Yellow compartments represent measured protein activity. Grey compartment represents measured cell viability. Black solid rectangles represent inhibition processes, while black open rectangles represent stimulation processes. Dashed arrows represent feedback loops.

Figure 2. Time course of cellular protein dynamics after continuous exposure of JIMT-1 cells to single agents: paclitaxel (50 nM), dasatinib (50 nM) and everolimus (50 nM) for 72 h. Relative protein expression profiles are shown for: *pSrc* (for dasatinib and everolimus), *pAkt* and *pmTOR* for all three agents, and *Caspase-3* activity for paclitaxel. Black circles represent observed data under control conditions, and red circles represent observed data under treatment conditions. Solid lines represent model fittings.

Figure 3. Time course of cellular protein dynamics after continuous exposure of JIMT-1 cells to combination therapies: DE simultaneous treatment with dasatinib+everolimus at 50 nM each, PDE simultaneous treatment with paclitaxel+dasatinib+everolimus at 50 nM each, and P_DE sequential treatment with paclitaxel (24 h prior)+(dasatinib+everolimus) at 50 nM each. Relative protein expression profiles are shown for *pSrc*, *pAkt*, *pmTOR* and *Caspase-3* activities for all combinations. Black circles represent observed data under control conditions, and red circles represent observed data under treatment conditions. Solid lines represent model fittings.

Figure 4. Time course of cellular viability response after continuous exposure of JIMT-1 cells to treatments with: paclitaxel (50 nM), dasatinib (50 nM), everolimus (50 nM), DE (50 nM each), PDE (50 nM each), and P_DE (50 nM each). Black circles represent observed data under control

conditions, and red circles represent observed data under treatment conditions. Solid lines represent model fittings.

Figure 5. Time course of cell viability response of JIMT-1 cells in the 3DD cell culture system. Black circles are observed data under control conditions, black solid profile is the model fitting for control data, red circles are observed data for P_DE treatment arm in the 3DD study, red solid profile is the model fitting for the P_DE treatment arm, blue profile is everolimus (50 nM for 72 h followed by washout), green profile is dasatinib (50 nM for 72 h followed by washout), orange profile is DE (50 nM for 72 h followed by washout), pink profile is paclitaxel (3 h short-term infusion followed by washout), yellow profile is paclitaxel (50 nM for 72 h followed by washout), purple dashed profile is PDE (50 nM for 72 h followed by washout for all three agents administered simultaneously), red dashed profile is P_DE (50 nM for 72 h with a 24 h interval between P and DE, followed by washout)

Figure 6. Time course of cell viability response of JIMT-1 cells in 3DD cell culture system for **A)** various treatment schedules and **B)** simulations over a longer duration (50 days). The simulated dosing regimens are: **black profile:** control arm, **blue profile:** everolimus (50 nM for 72 h followed by washout), **green profile:** dasatinib (50 nM for 72 h followed by washout), **orange profile:** DE (50 nM each for 72 h followed by washout), **pink profile:** paclitaxel (3 h short-term infusion) **yellow profile:** paclitaxel (50 nM for 72 h followed by washout), **purple dashed profile:** PDE (50 nM of each agent administered for 72 h followed by washout), **red dashed profile:** P_DE (50 nM of each agent administered for 72 h; 24 h interval), **green dashed profile:** P_DE (50 nM of each agent administered for 72 h; 48 h interval), **yellow dashed profile:** P_DE (50 nM of each agent administered for 72 h; 72 h interval), **blue dashed profile:** P_DE (50 nM of each agent administered for 72 h; 96 h interval), **orange dashed profile:** P_DE (50 nM of each agent administered for 72

JPET Fast Forward. Published on March 21, 2019 as DOI: 10.1124/jpet.118.255752
This article has not been copyedited and formatted. The final version may differ from this version.

h; 120 h interval), **grey dashed profile:** P_DE (25 nM of each agent administered for 72 h; 24 h interval), **black dashed profile:** PDE (25 nM of each agent administered for 72 h simultaneously)

JPET Fast Forward. Published on March 21, 2019 as DOI: 10.1124/jpet.118.255752
This article has not been copyedited and formatted. The final version may differ from this version.

Table 1: Parameter estimates for protein network dynamics and cellular response models for JIMT-1 cells in the 2D and 3DD systems

Parameter (Unit)	Definition	Estimate	Relative Standard Error (% RSE)
Turnover of Measured Signaling Proteins			
K_{src} (h^{-1})	Turnover rate constant for pSrc	0.237	17
K_{Akt} (h^{-1})	Turnover rate constant for pAkt	3.37	34
K_{mTOR} (h^{-1})	Turnover rate constant for pmTOR	0.094	22
K_{cas} (h^{-1})	Turnover rate constant for active caspase-3	0.02	12
Paclitaxel Model Parameters – 2D System			
K_{inh} (h^{-1})	Turnover rate constant for pAkt inhibitory compartment	0.708	26
Ip (x 10^{-1} nM^{-1})	Coefficient of pAkt inhibition by Paclitaxel	0.173	9
($1/\tau_{MP}$) (x10^{-1} h^{-1})	Transit rate constant for effect of pAkt on pmTOR due to Paclitaxel	0.567	11
$S1_P$	Coefficient of inhibition of pmTOR	1[a]	-
($1/\tau_{CP}$) (x 10^{-1} h^{-1})	Transit rate constant for activation of caspase-3 due to Paclitaxel	0.697	16
k_P (nM^{-1})	Slope for activation of caspase-3	1[b]	-
$S2_P$	Exponent for activation of caspase-3	0.445	18
$S3_P$	Feedback coefficient for active caspase-3	15.3	66
$S4_P$	Coefficient of paclitaxel-mediated cell growth inhibition due to pmTOR	1[a]	-
kg (x 10^{-1} h^{-1})	Net growth rate constant for JIMT-1 cells	0.089	5
kd_P (h^{-1})	Death rate constant for JIMT-1 cells due to Paclitaxel	0.123	3
Dasatinib Model Parameters – 2D System			
$S1_D$ (x 10^{-1} nM^{-1})	Coefficient of pSrc inhibition by Dasatinib	0.181	2
$S2_D$	Coefficient of inhibition of pAkt due to pSrc	0.293	28
($1/\tau_{MD}$) (x 10^{-1} h^{-1})	Transit rate constant for effect of pAkt on pmTOR due to Dasatinib	0.701	40
$S3_D$	Coefficient of inhibition of pmTOR	4.76	41
kg (x 10^{-1} h^{-1})	Net growth rate constant for JIMT-1 cells	0.089	5
$S4_D$	Coefficient of dasatinib-mediated cell growth inhibition due to pmTOR	10.9	36
Everolimus Model Parameters – 2D System			
$S1_E$ (x 10^{-1} nM^{-1})	Coefficient of pmTOR inhibition by Everolimus	0.151	4

JPET Fast Forward. Published on March 21, 2019 as DOI: 10.1124/jpet.118.255752
This article has not been copyedited and formatted. The final version may differ from this version.

$S2_E$	Coefficient for effect of pAkt on pmTOR	1.42	8
$(1/\tau_{SE})$ (h^{-1})	Transit rate constant for feedback activation effect of pmTOR on pSrc	1	66
$S3_E$	Coefficient of feedback activation of pSrc due to pmTOR	7.27	65
$S4_E$	Coefficient of feedback activation of pAkt due to pmTOR	1[a]	-
$S5_E$	Coefficient of effect of pSrc on pAkt	1[a]	-
kg (x 10^{-1} h^{-1})	Net growth rate constant for JIMT-1 cells	0.089	5
$S6_E$	Coefficient of everolimus-mediated cell growth inhibition due to pmTOR	0.001[c]	-
Dasatinib+Everolimus Model Parameters – 2D System			
$S1_{DE}$	Coefficient for effect of pAkt on pmTOR	1.36	34
$(1/\tau_{CDE})$ (h^{-1})	Transit rate constant for activation of caspase-3 due to Dasatinib+Everolimus (D+E)	0.996	2
k_{DE} (nM^{-1})	Slope for activation of caspase-3	1[b]	-
$S2_{DE}$	Exponent for activation of caspase-3	2.06	10
$S3_{DE}$ (x 10^{-1})	Signal modulation coefficient for caspase-3 activation	0.262	42
kg (h^{-1})	Net growth rate constant for JIMT-1 cells	0.009	5
$S4_{DE}$	Coefficient of D+E – mediated cell growth inhibition due to pmTOR	1[a]	-
kd_{DE} (h^{-1})	Death rate constant for JIMT-1 cells due to D+E	0.124	10
Paclitaxel+Dasatinib+Everolimus Simultaneous Treatment Model Parameters – 2D System			
$S1_{PDE}$	Coefficient for effect of pAkt on pmTOR	4.71	14
$S2_{PDE}$	Coefficient for feedback effect on pAkt due to pmTOR	1	-
$(1/\tau_{CPDE})$ $(x10^{-1}h^{-1})$	Transit rate constant for activation of caspase-3 due to Paclitaxel+Dasatinib+Everolimus (P+D+E)	0.128	29
kg (h^{-1})	Net growth rate constant for JIMT-1 cells	0.009	6
$S3_{PDE}$	Coefficient of P+D+E – mediated cell growth inhibition due to pmTOR	1[a]	-
kd_{PDE} (x 10^{-1} h^{-1})	Death rate constant for JIMT-1 cells due to P+D+E	0.786	3
Paclitaxel+(Dasatinib+Everolimus) Sequential Treatment Model Parameters – 2D System			
$S2_{P(DE)}$	Coefficient for feedback effect on pAkt due to pmTOR	0.0943	17
$S1_{P(DE)}$	Coefficient for effect of pAkt on pmTOR	1.01	27
kg (h^{-1})	Net growth rate constant for JIMT-1 cells	0.009	6
$S4_P$	Coefficient of P mediated cell growth inhibition due to pmTOR (prior to 24 h)	1[a]	-
$S3_{PDE}$	Coefficient of PDE mediated cell growth inhibition due to pmTOR (post 24 h)	1[a]	-

JPET Fast Forward. Published on March 21, 2019 as DOI: 10.1124/jpet.118.255752
This article has not been copyedited and formatted. The final version may differ from this version.

kd_P (x 10^{-1} h^{-1})	Death rate constant for JIMT-1 cells due to P (prior to 24 h)	0.774	4
kd_{PDE} (h^{-1})	Death rate constant for JIMT-1 cells due to PDE (post 24 h)	0.124	10
Paclitaxel+(Dasatinib+Everolimus) Sequential Treatment Model Parameters - 3DD System			
λ_0 (x10^{-2} h^{-1})	Rate constant for exponential growth of JIMT-1 cells	0.77	5
λ_1 (h^{-1})	Rate constant for linear growth of JIMT-1 cells	7.41	59
Ψ	Switching factor between exponential and linear growth	20[d]	-
α_P	Coefficient for JIMT-1 growth inhibition due to pmTOR (prior to 24 h)	1	23
β_P (h^{-1})	Death rate constant for JIMT-1 due to caspase-3 activity (prior to 24 h)	0.132	3
α_{PDE}	Coefficient for JIMT-1 growth inhibition due to pmTOR (post 24 h)	1	23
β_{PDE} (x 10^{-1} h^{-1})	Death rate constant for JIMT-1 due to caspase-3 activity (post 24 h)	0.841	3
Scaling Factors for Translation of 2D Models to the 3DD System			
$\alpha_P/S4_P$, $\alpha_{PDE}/S2_{PDE}$	Ratio of cell growth inhibition coefficients in 3DD and 2D	1	-
β_P/kd_P, β_{PDE}/kd_{PDE}	Ratio of cell death rate constants in 3DD and 2D systems	1.07	-

[a] Coefficients were fixed to 1 to indicate a direct/inverse proportionality (as applicable) to the actual magnitude of the activity of a particular protein, without the need of a power coefficient.

[b] Slopes (proportionality constants) were fixed to 1 as the exponents used to characterize activation of caspase-3 due to drug concentrations alone were sufficient

[c] Coefficient fixed to a relatively low magnitude to indicate minimal effect of activity of a protein. Any decrease in magnitude of this coefficient did not have an impact on model fittings.

[d] Fixed factor to allow for a smooth switch from exponential to linear cell growth (Magni et al., 2006)

JPET Fast Forward. Published on March 21, 2019 as DOI: 10.1124/jpet.118.255752
This article has not been copyedited and formatted. The final version may differ from this version.

Table 2. Time to tumor re-growth (TTR)[a] of JIMT-1 cells for dosing regimens simulated in the 3DD system **(Figure. 6B)**

Dosing Regimen	**Profile color in fig. 6B**	**TTR (days)**
Everolimus (50 nM for 72 h followed by washout)[b]	Blue	-
Dasatinib (50 nM for 72 h followed by washout)	Green	2.2
DE (50 nM for 72 h followed by washout)	Orange	6.1
Paclitaxel (3 h short-term infusion)	Pink	8.6
Paclitaxel (50 nM for 72 h followed by washout)	Yellow	10.9
P(DE) sequential (120 h interval; 50 nM 72 h)	Orange dashed	15.4
P(DE) sequential (96 h interval; 50 nM 72 h)	Blue dashed	15.5
P(DE) sequential (24 h interval; 50 nM 72 h)	Red dashed	24.3
P(DE) sequential (48 h interval; 50 nM 72 h)	Green dashed	26.0
P(DE) sequential (72 h interval; 50 nM 72 h)	Yellow dashed	26.8
PDE simultaneous (50 nM, 72 h)	Purple dashed	24.6
P(DE) sequential (24 h interval; 25 nM for 72 h followed by washout)	Grey dashed	23.1
PDE simultaneous (25 nM for 72 h followed by washout)	Black dashed	22.9

a TTR was calculated as the horizontal distance between the control arm (black) and treatment profiles, when all growth curves became nearly parallel to one another after cessation of treatment

b TTR for everolimus was not calculated due to lack of a significant cytostatic/cytotoxic effect. Its profile nearly overlapped with the control profile.

JPET Fast Forward. Published on March 21, 2019 as DOI: 10.1124/jpet.118.255752
This article has not been copyedited and formatted. The final version may differ from this version.

Figure 1

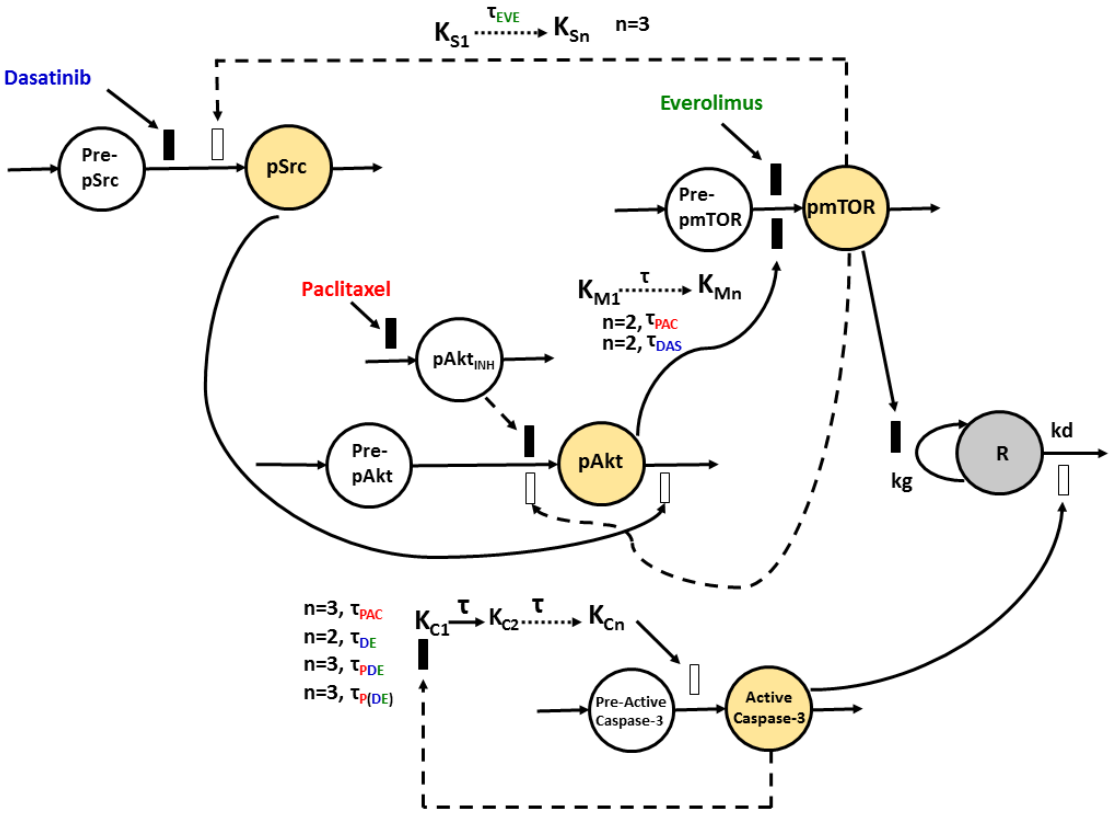

JPET Fast Forward. Published on March 21, 2019 as DOI: 10.1124/jpet.118.255752
This article has not been copyedited and formatted. The final version may differ from this version.

Figure 2

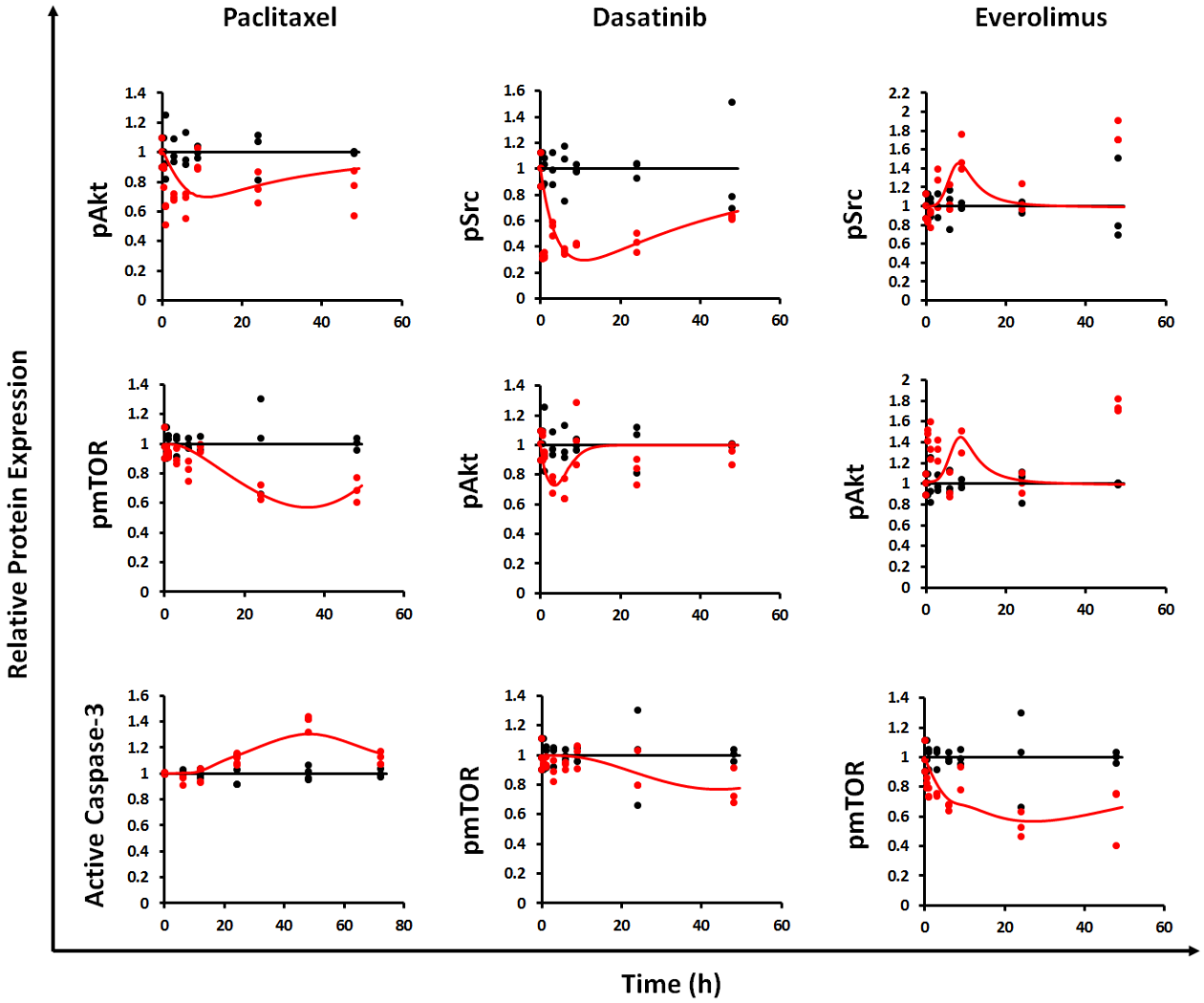

JPET Fast Forward. Published on March 21, 2019 as DOI: 10.1124/jpet.118.255752
This article has not been copyedited and formatted. The final version may differ from this version.

Figure 3

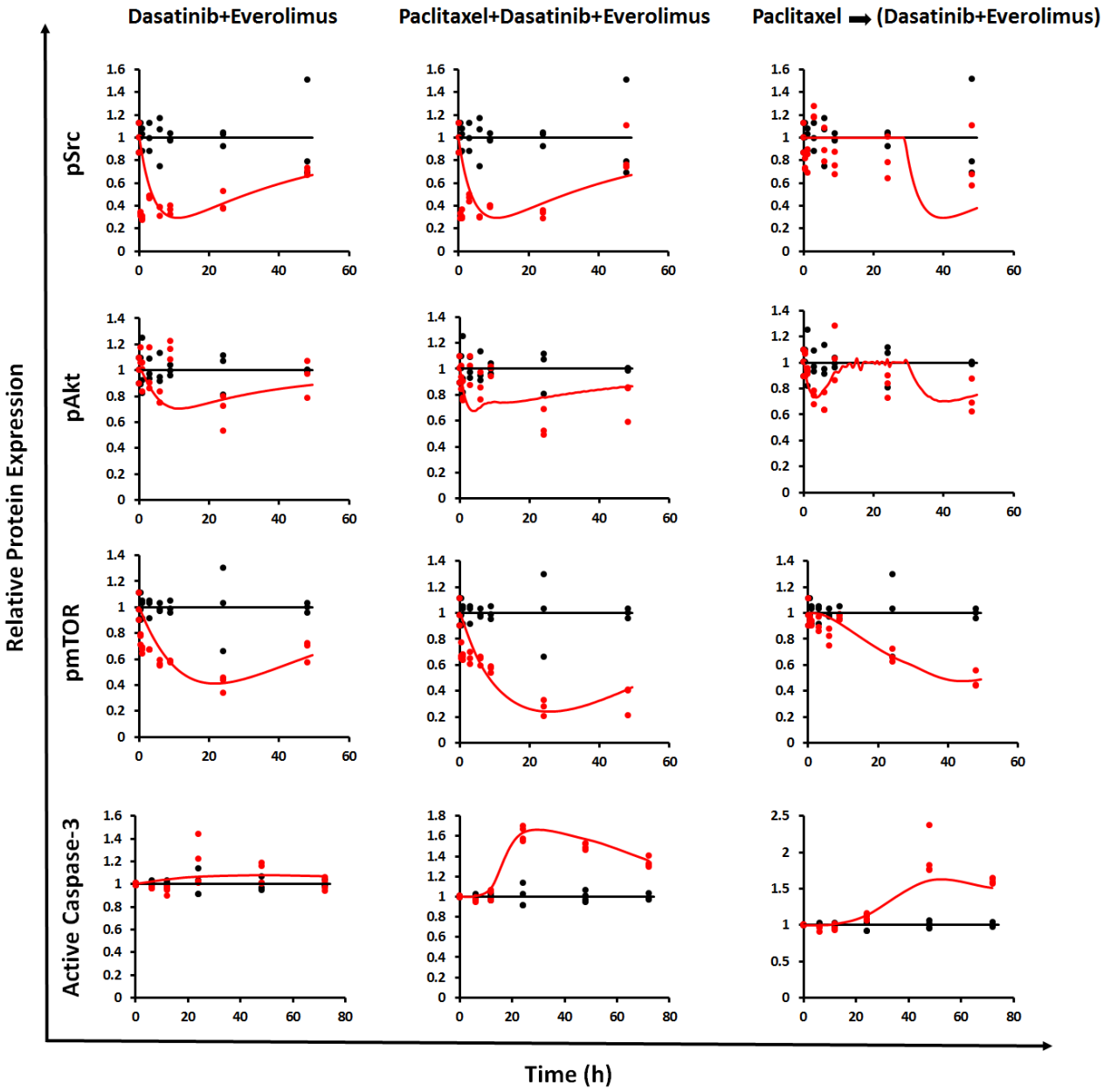

JPET Fast Forward. Published on March 21, 2019 as DOI: 10.1124/jpet.118.255752
This article has not been copyedited and formatted. The final version may differ from this version.

Figure 4

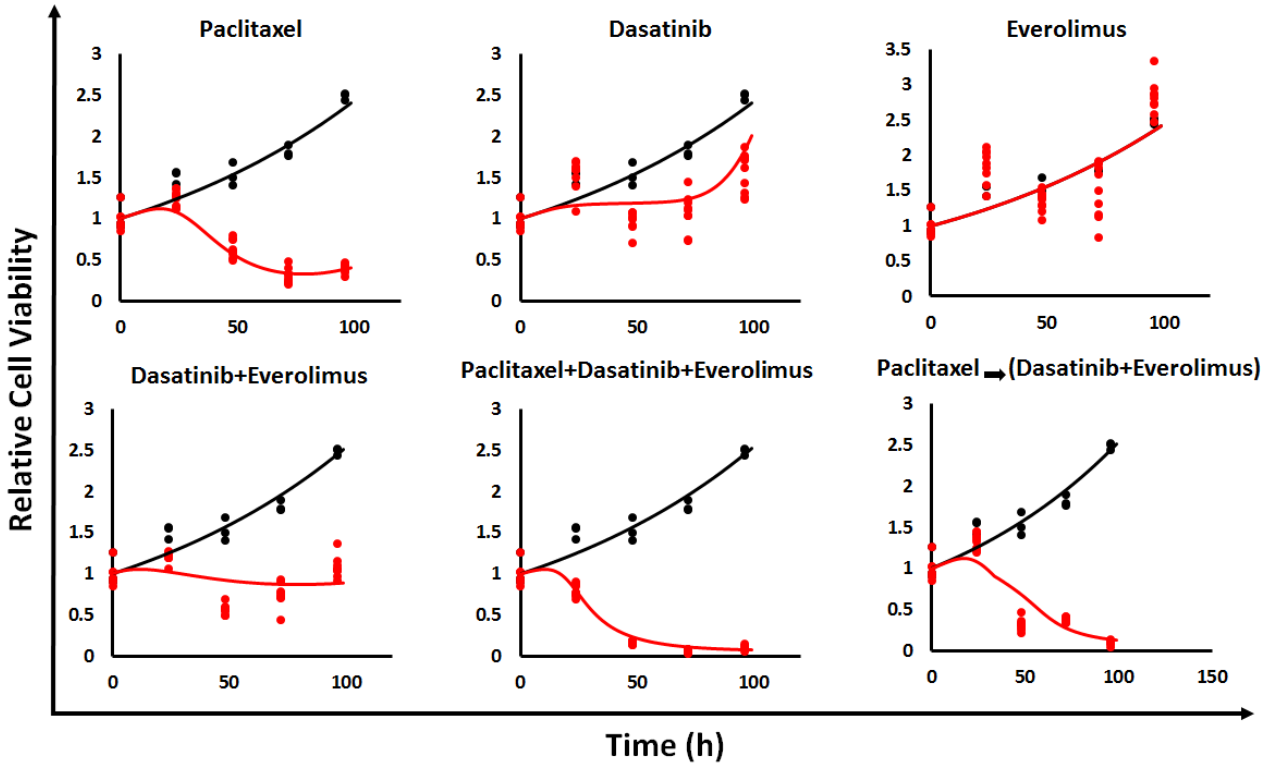

JPET Fast Forward. Published on March 21, 2019 as DOI: 10.1124/jpet.118.255752
This article has not been copyedited and formatted. The final version may differ from this version.

Figure 5

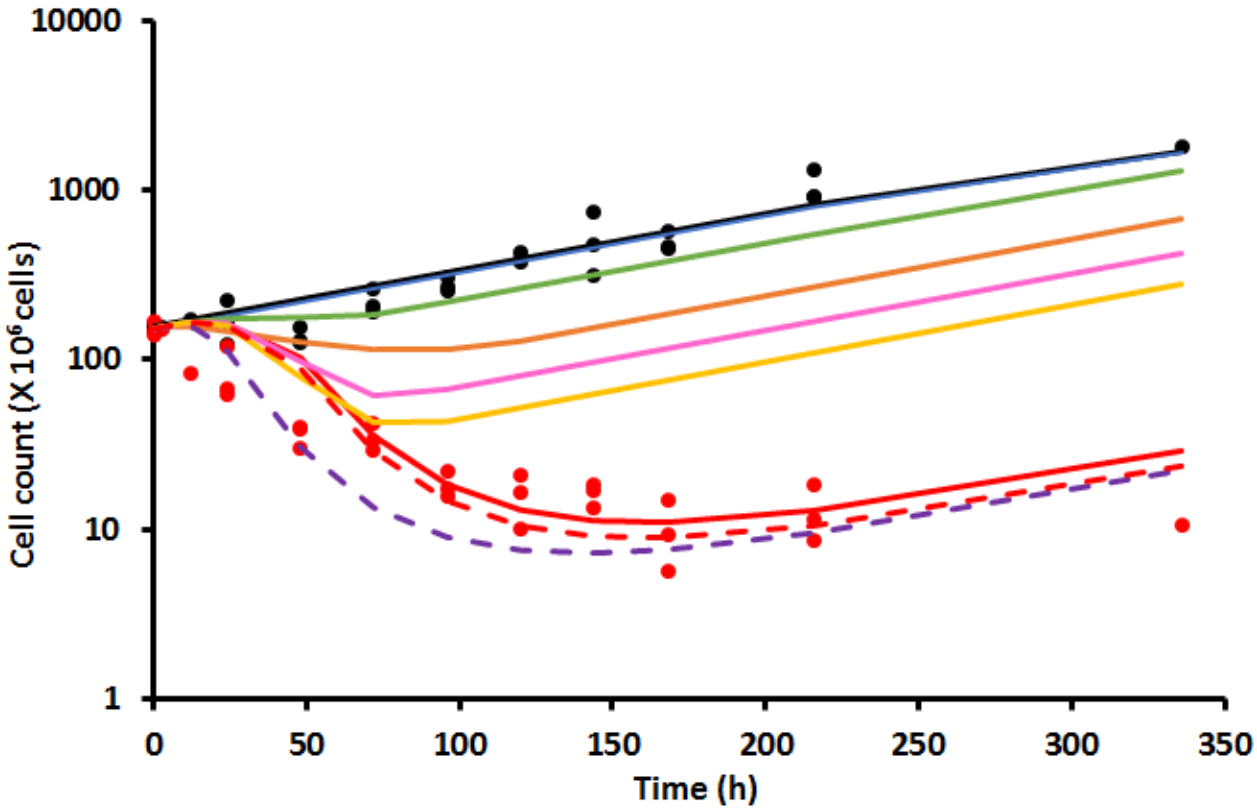

JPET Fast Forward. Published on March 21, 2019 as DOI: 10.1124/jpet.118.255752
This article has not been copyedited and formatted. The final version may differ from this version.

Figure 6